ISSN: 1813-1786
Volume No. 19
Indexed & Abstract in:
- PASTIC SCIENCE ABSTRACTS
- AGRIS DATABASE
- ProQuest Products

TECHNICAL JOURNAL

2014

University of Engineering and Technology Taxila

Vol: 19 No. II (Apr - June)

Technical Journal

A Quarterly Journal of University of Engineering & Technology, Taxila
Recognized by Higher Education Commission (HEC)
Y Category

ISSN: 1813-1786
Volume No. 19
No. II (Apr - June)
2014

Phone: 92 - 51 - 9047455 **Fax: 92 - 51 - 9047420** **E-Mail: technical.journal@uettaxila.edu.pk**

Technical journal is abstracted and indexed in ProQuest Products, Agris, Pakistan Science abstract, Ulrich periodic directory plus Pastic indexing service.

EDITORIAL OFFICE:
Librarian/Managing Editor Technical Journal
Central Library, University of Engineering and Technology, Taxila

EDITORIAL BOARD

CONTENTS

Experimental Determination of Mechanical Quality Factor of Lead Zirconate Titanate (PZT-5A4E) by Equivalent Circuit Method under various Thermal and Resistance Conditions

H. Elahi[1], R. A. Pasha[2], M. Z. Khan[3]

[1]Mechanical Engineering Department UET Taxila, Pakistan
[2]Mechanical Engineering Department UET Taxila, Pakistan
[3]Mechanical Engineering Department IST Islamabad, Pakistan
[1]hassanelahi_uet@yahoo.com
[2]asim.pasha@uettaxila.edu.pk
[3]zubair.khan@ist.edu.pk

Abstract-Piezoelectric effect is a linear electromechanical effect between electrical and mechanical properties. In this research work, a specially designed apparatus was used to determine the mechanical quality factor of Lead Zirconate Titanate (PZT-5A4E) by shocking it at variable frequencies and resistances under various thermal conditions. Equivalent circuit method was used to determine the mechanical quality factor by shocking it at resonant frequency and anti-resonant frequency. It was found that with the increase in temperature and resistance mechanical quality factor decreases.

Keywords-PZT-5A4E, Resistance, Electromechanical Interaction, Frequency, Thermal Conditions.

I. INTRODUCTION

PIEZOELECTRIC materials are those which on the application of mechanical stress can produce electric voltage. Out of 32 known crystalline groups, 28 are piezoelectric in nature. The macroscopic behavior of the piezoelectric materials differs from that of individual crystallites, due to orientation of such crystallites [1]. The technique to convert mechanical input to electric output with the help of piezoelectric vibrator was developed [2]. Mechanical quality factor was declared as one of the most basic parameters for piezoelectric materials [3]. Piezoelectric materials are versatile that makes them unique from other crystals [4]. Thermal expansion is useful technique in piezoelectric materials rather than other solid materials [5]. Reference [6] determined mechanical impedance of piezoelectric material from the electrical impedance. Electric voltage generated by piezoelectric material depends on its boundary conditions as well as on its electrical conductivity [7]. Increase in the pressure applied causes reduction in piezoelectric area [8]. Reference [9] analyzed piezoelectric ring with high mechanical quality factor as a transformer at different temperatures to increase its efficiency at varying load conditions. Reference [10] optimized multi-layer newly doped factor that resonate at 1.7MHz and have a lot of applications as sensors and actuators. A new class of piezoelectric materials was introduced having high quality material for high power applications and high temperature applications [11]. Reference [12] developed piezoelectric materials and increased their mechanical quality factor at sintering temperature. Trends and behavior of a piezoelectric material as a ceramic at different temperatures were shown [13]. Reference [14] determined dynamic characteristic of piezoelectric material.

Our aim was to find out the mechanical quality factor at variable temperatures and resistances. Now a days field of Micro Electro Mechanical System is emerging, piezoelectric materials as a sensor and actuator has a vast role in it, so there characterization also plays a vital role in this field for smart structures.

II. MATERIAL

Lead zirconate titanate is a ceramic material that shows remarkable piezoelectric effect as compared to other ferroelectric properties. PZT develops a voltage difference across two of its faces when compressed (mostly used in sensor applications), and physically strained when an external electric field is applied (used for actuators etc). It is also ferroelectric, in other words, it has a spontaneous polarization which can be reversed in the presence of an electric field. The lead zirconate titanate is widely used in polycrystalline (ceramic) with very high piezoelectric coupling. Depending on the formula of preparation, PZT materials may have different forms and properties. Manufacturers of PZT use proprietary formulas for their products. Techniques

that are commonly used for preparing the bulk PZT materials such as (PZT-4, PZT-5) are not suited for micro-fabrication. A number of techniques for preparing PZT films have been demonstrated, including sputtering, laser ablation, jet molding, and electrostatic spray deposition. Lead zirconate titanate shows much greater piezoelectricity effect than quartz. These can readily be fabricated into variety of shapes and sizes and therefore can be tailored to a particular application. Dimensions of the specimen used are provided in Table I while the piezoelectric, mechanical and thermal properties are provided in Table II.

TABLE I
DESCRIPTION OF SPECIMEN (PZT-5A4E SINGLE LAYER DISKS)

Composition	Trade	(Dimension)		Part No
		Diameter	Thickness	
Lead Zirconate Titanate	PiezoSystems Inc.	12.7mm	0.191mm	T107-A4E-273

TABLE II
PARENT SPECIMEN PROPERTIES

Piezoelectric Properties				
Sr #	Description	Notation	Value	Units
01	Relative Dielectric Constant @1KHz	K^T_3	1800	
02	Piezoelectric strain coefficient	d_{33}	390 x10^{-12}	Meters/Volt
03		d_{31}	-190 x 10^{-12}	Meters/Volt
04	Piezoelectric voltage coefficient	g_{33}	24 x 10^{-3}	Volt meters/Newton
05		g_{31}	-11.6 x 10^{-3}	Volt meters/Newton
06	Coupling coefficient	K_{33}	0.72	
07		k_{31}	0.32	
08	Polarization field	E_p	2 x 10^6	Volts /meter
09	Initial depolarization field	E_c	5 x 10^5	Volts/meter
Mechanical				
10	Density	P	7800	Kg/meter^3
11	Mechanical Q	Q	80	
12	Elastic modules	Y^E_3	5.2 x 10^{10}	Newtons/meter^2
13		Y^E_1	6.6 x 10^{10}	Newtons/meter^2
Thermal				
14	Thermal expansion coefficient		~ 4 x 10^{-6}	Meters/meter ^oC
15	Curie Temperature		350	^oC

III. EXPERIMENTAL SETUP

The experimental setup consisted of a load cell fixed with the base of mild steel sheet, the square shaped specimen was fixed with nut and bolt on the load cell in such a way that it's lower and upper both sides face copper electrodes as anode and cathode. To perform electrical and thermal insulation mica sheet was used which is resistant to both electrical and thermal conductivity. For the sake of on spot heating we used heat filament element in a circuit and to observe the temperature, temperature gun is used. The response is analyzed on digital oscilloscope at different temperatures. Experimental setup and overall circuit diagram are shown in Fig. 1 and Fig. 2 respectively.

Fig.1. Experimental Setup

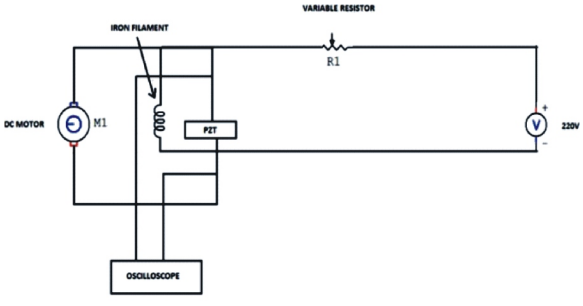

Fig. 2. Circuit diagram for the experimental setup

We applied sinusoidal waveform to shock the piezoelectric material.

The calculations for prediction of mechanical quality factor are given in equations 1, 2, and 3.

$$Qm=Xc/R \quad (1)$$

As impedance is

$$Xc= 1/(2\pi fC) \quad (2)$$

So eq. (1) Becomes

$$Qm=1/(2\pi fRC) \quad (3)$$

Where "f" is average frequency of resonant frequency fa and anti-resonant frequency fb. As shown in Fig. 3.

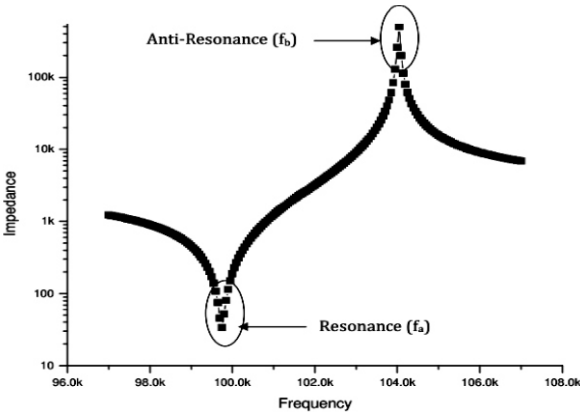

Fig. 3. Impedance curve of piezoelectric material showing resonance and anti-resonance

IV. Results And Discussions

Experiments were performed at variable temperatures ranging from 20 °C to 200 °C. The mechanical quality factor was found to be decreased with the increase in temperature showing 2nd order polynomial behavior as shown in Fig. 4.

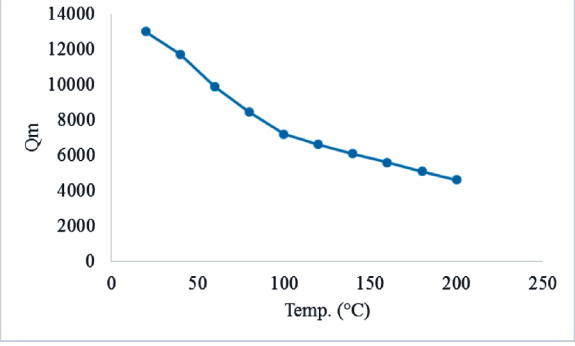

Fig. 4. Prediction of Mechanical Quality Factor of a piezoelectric material under variable Temperature

It is observed that on increasing the resistance at constant temperature conditions (initially at 20 °C and then at 100 °C, the mechanical quality factor decreases accordingly. Resistance was varied from 5 K ohm to 82 K ohm and its response was observed on the oscilloscope. 3rd order polynomial behavior was observed as shown in Fig. 5 and Fig. 6.

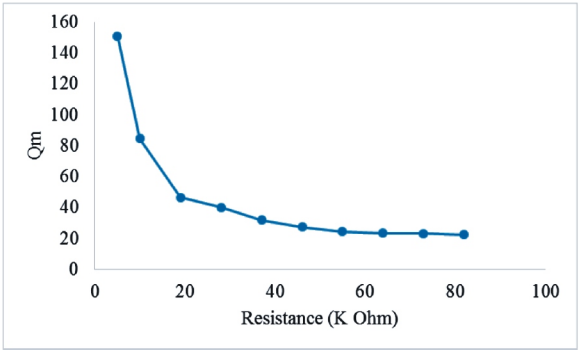

Fig. 5. Mechanical Quality Factor of a piezoelectric material under 20°C Temperature and Variable Resistance

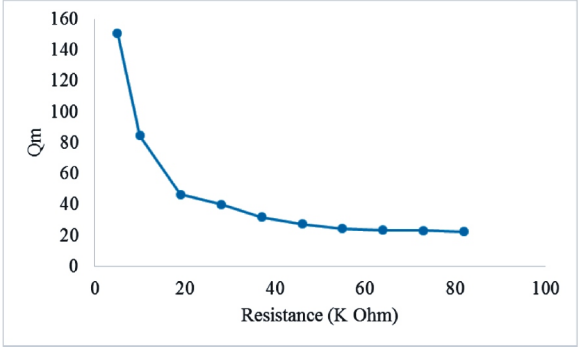

Fig. 6. Mechanical Quality Factor of a piezoelectric material under 100°C Temperature and Variable Resistance

Similar behavior was observed at a constant temperature of 180°C as shown in Fig. 7.

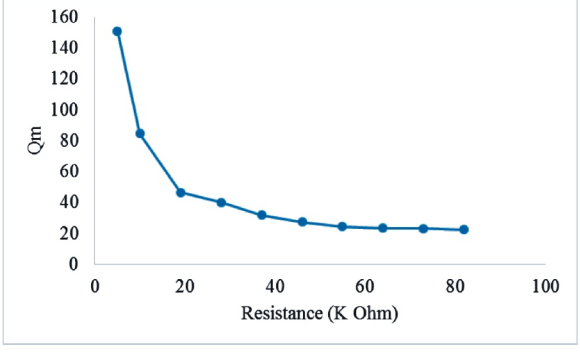

Fig. 7. Mechanical Quality Factor of a piezoelectric material under 180°C Temperature and Variable Resistance

V. Conclusions

Following are the conclusions obtained from the current research work:

1. With the increase in temperature up to Curie temperature the mechanical quality factor of Lead Zirconate Titanate decreases as a linear function.

2. Negative linear behaviour is observed between temperature and Qm as well as for resistance because effect of polarization.
3. For best performance and for maximum mechanical quality factor use pzt at 20 °C temperature, 0 Ohm resistance, and 200 Hz frequency because of dipolar motion of its ions. So it is highly applicable to use Lead Zirconate Titanate at low temperature, low resistance and high frequency for maximum results.

REFERENCES

[1] C. Liu, Foundation of MEMS. Electrical and computer Department University of Illionis at Urbana-Champaign Pearson Education International, 2006.

[2] W. L. Bond, PIEZOELECTRIC VIBRATOS. 1947, Google Patents.

[3] F. R. M. D. Espinosa, J. L. S. Emeterio and P.T. Sanz, Summary of the measurement methods of Qm for piezoelectric materials. Ferroelectrics, 1992. 128(1): p. 61-66.

[4] G. Feuillard et al. Experimental determination of SAW properties of 5 standard piezoceramics in Ultrasonics Symposium, 1994. Proceedings. 1994 IEEE.

[5] Y. Yamagata et al. A micro mobile mechanism using thermal expansion and its theoretical analysis. A comparison with impact drive mechanism using piezoelectric elements in Micro Electro Mechanical Systems, 1994, MEMS'94, Proceedings, IEEE Workshop.

[6] Y. Deblock et al. The determination of the viscoelastic properties of liquid materials at ultrasonic frequencies by CW mode impedance measurements. Instrumentation and Measurement, IEEE Transactions on, 1998. 47(3): p. 680-685.

[7] A. Giannakopoulos and S. Suresh, Theory of indentation of piezoelectric materials. Acta materialia, 1999. 47(7): p. 2153-2164.

[8] J. Sferruzza, A. Birer and D. Cathignol, Generation of very high pressure pulses at the surface of a sandwiched piezoelectric material. Ultrasonics, 2000. 38(10): p. 965-968.

[9] J. H. Hu et al. A ring-shaped piezoelectric transformer operating in the third symmetric extensional vibration mode. Sensors and Actuators A: Physical, 2001. 88(1): p. 79-86.

[10] Y. Hou, Piezoelectric properties of new MnO2-added 0.2 PZN0.8 PZT ceramic. Materials Letters, 2004. 58(9): p. 1508-1512.

[11] G. Piazza et al. Voltage-tunable piezoelectrically-transduced single-crystal silicon micromechanical resonators. Sensors and Actuators A: Physical, 2004. 111(1): p. 71-78.

[12] S. Zhang et al. Piezoelectric materials for high power, high temperature applications. Materials Letters, 2005. 59(27): p. 3471-3475.

[13] A. Moure, A. Castro and L. Pardo, Aurivillius-type ceramics, a class of high temperature piezoelectric materials: Drawbacks, advantages and trends. Progress in Solid State Chemistry, 2009. 37(1): p. 15-39.

[14] Y. A. Zhuk, I. A. Guz and C.M. Sands, Monoharmonic approximation in the vibration analysis of a sandwich beam containing piezoelectric layers under mechanical or electrical loading. Journal of Sound and Vibration, 2011. 330(17): p. 4211-4232.

Determination of Fretting Fatigue Behavior in Titanium Alloy Ti-6Al-4V: A review

Z. Anjum[1], M. Shah[2], S. Ahmed[3]

[1]Mechanical Engineering Department UET Taxila, Pakistan
[2]Mechanical Engineering Department UET Taxila, Pakistan
[3]Mechanical Engineering Department UET Taxila, Pakistan
[1]zeeshan-89@hotmail.com
[2]masood.shah@uettaxila.edu.pk
[3]sagheer.ahmad@uettaxila.edu.pk

***Abstract*-**Fretting fatigue is an important concern in the structures and machine parts that are subjected to repeated relative movements between them. In current study a review of the work done by various researchers related to the evaluation of fretting fatigue response of Ti-6Al-4V has been presented. Effects of surface treatments, crack growth, heat treatments, types of loading, contact pad configuration on the fretting fatigue life have been presented. Life prediction models developed by various researchers have also been discussed.

***Keywords*-**fretting fatigue, review, Ti-6Al-4V, crack growth, heat treatment.

I. Introduction

Fretting fatigue failure is a type of failure which occurs in structures and machine parts, typically in gas turbine disc and blade joints, due to vibration between them. Titanium after being alloyed with aluminum, vanadium and other elements is highly suitable to be used in aircraft, naval ships, armor plating, missiles and aircrafts because of high strength to weight ratio, higher capability to resist corrosion. Most importantly it resists the crack growth and creep elongation even at high temperatures. Ti-6Al-4V is the mostly used alloy in aircraft applications, almost 50% of all alloys [1]. Composition of Ti-6Al-4V alloy and its physical, mechanical, electrical and thermal properties are given in Table I and Table II respectively.

TABLE I
Composition of Ti-6Al-4V. [2]

Component	Weight (%)
Al	6
Fe	Max 0.25
O	Max 0.2
Ti	90
V	4

TABLE II
Physical, Mechanical, Electrical And Thermal Properties Of Ti-6Al-4V. [2]

Physical *Properties*	Metric	Imperial
Density	4.43 g/cc	0.16 lb/in^3
Mechanical Properties		
Hardness, Brinell	334	334
Hardness, Knoop	363	363
Hardness, Rockwell C	36	36
Hardness, Vickers	349	349
Tensile Strength, Ultimate	950 MPa	138000 psi
Tensile Strength, Yield	880 MPa	128000 psi
Modulus of Elasticity	113.8 GPa	16500 ksi
Compressive Yield Strength	970 MPa	141000 psi
Notched Tensile Strength	1450 MPa	210000 psi
Ultimate Bearing Strength	1860 MPa	270000 psi
Poisson's Ratio	0.342	0.342
Charpy Impact	17J	12.5 ft-lb
Fracture Toughness	75 MPa-m½	68.3 ksi-in½
Shear Strength	550 MPa	79800 psi
Shear Modulus	44 GPa	6380 ksi
Electrical Properties		
Electrical Resistivity	0.000178 ohm-cm	0.000178 ohm-cm
Magnetic Permeability	1.00005	1.00005
Magnetic Susceptibility	3.3e-006	3.3e-006
Thermal Properties		
Thermal Conductivity	6.7 W/m-k	46.5 BTU-in/hr-ft^2-°F
Specific Heat Capacity	0.5263 J/g-°C	0.126 BTU/lb-°F
Melting Point	1604-1660 °C	2920-3020 °F

II. REVIEW

2.1 Surface Treatments

The purpose of surface finishing/ treatments is to acquire desired improved properties in the manufactured parts like wear and damage resistance, resistance to corrosion, reducing stress concentration, hardness, appearance and increasing the total life of the part.

Reference [3] found that by the application of different coating processes and surface treatments: shot peening, ion-beam-enhanced deposition (IBED) CrN films, shot-peening + IBED CrN films and IBED CuNiIn films on Ti-6Al-4V specimens, their resistance to fretting wear damage and fatigue strength can be enhanced as shown in Fig. 1 and Fig. 2. They found that IBED CrN films exhibit the highest resistance to fretting fatigue however duplex treatment by shot-peening/IBED CrN exhibit superior resistance towards fretting wear.

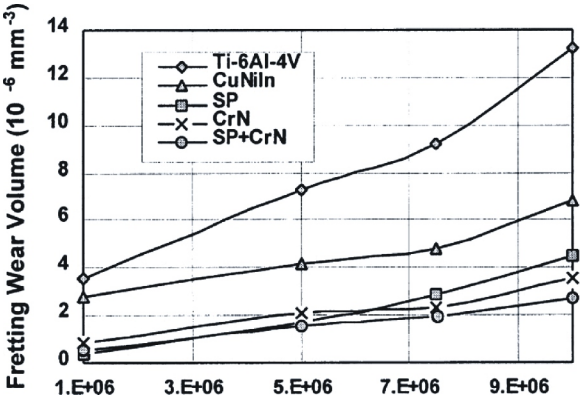

Fig. 1. Graph showing the comparison of the fretting wear volume for various surface treatments at 20 N load and 50 μm slip amplitude. [3]

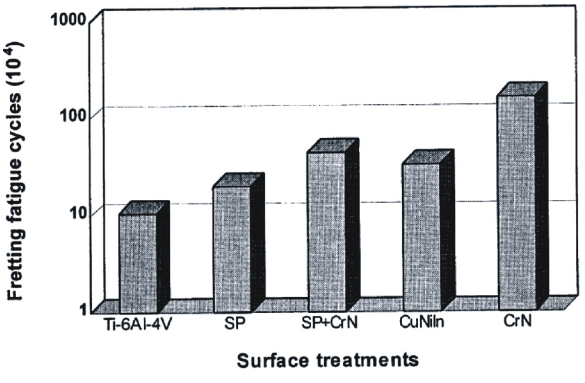

Fig. 2. Comparison of fretting fatigue strength by the application of different surface treatments. [3]

Reference [4] conducted an experimental study to analyze the response of Ti-6Al-4V specimen in contact with pads under four surface conditions: Ti-6Al-4V (bare) with highly polished surface, Ti-6Al-4V (bare) grit blasted to RMS #64, Ti-6Al-4V polished to RMS #8 and Ti-6Al-4V plasma spray coated with Cu-Ni. 20-25% increase in fretting fatigue strength was found for Cu-Ni plasma spray coated specimens as compare to those polished to RMS #8. The response of Ti-6Al-4V specimens against above four treatments was also evaluated using fatigue tests and S-N curves. It was found that the mechanism responsible for improving fretting fatigue strength was surface roughness rather than material of the parts in contact with each other.

Reference [5] studied the effect of re-shot peening on fretting fatigue strength of forged and previously shot-peened Ti-6Al-4V specimens at room temperature and at elevated temperatures. Relaxed residual stresses were found to be successfully recovered to a level of initial shot peening by the re-shot peening process. 20-25% residual stress relaxation was induced by the conditions applied during their study. Further re-shot peening eliminated the effects of any damage caused by fretting fatigue after initial shot peening.

Reference [6] studied the potential of four coating systems (TiCN, CrN+MoS_2, Cu-Al and Ag+ irradiated layer) towards enhancing the fretting fatigue strength of Ti-6Al-4V specimens. Fretting lives and coefficient of friction of both coated and without coating were compared as shown in Fig. 3 and Fig. 4 respectively. Finally the tested specimens were analyzed using Scanning Electron Microscope (SEM) and energy dispersive spectrometry for understanding the microstructural information about coating degradation process.

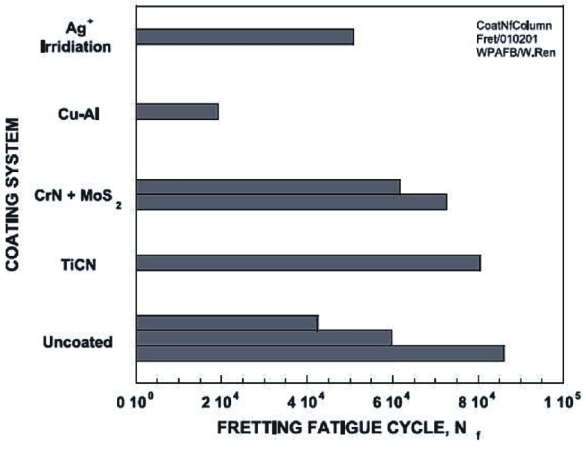

Fig. 3. Comparison of fretting fatigue lives under different coating conditions. [6]

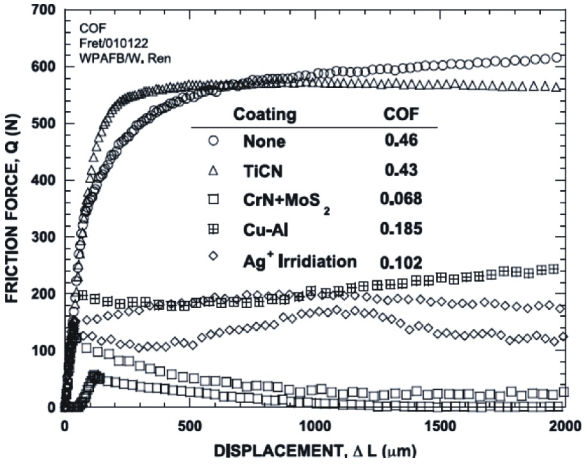

Fig. 4. Comparison of coefficient of friction of different coating systems. [6]

Reference [7] conducted the fretting fatigue tests of Ti-6Al-4V specimens which were initially shot peened by the application of independent pad displacement using dual actuator setup at a certain applied stress under slip controlled mode and found that fretting regime changes from partial to mixed mode slip and then by increasing the relative slip upto 50 μm it changes into gross slip. Due to compressive residual stresses the fretting fatigue life of shot-peened specimen was found to be longer than un-peened at the same slip range.

Investigation on the fretting fatigue response of Ti-6Al-4V specimens and pads using two different experimental setups and five coating systems resulted that the specimens with DLC coatings and LSP and LPB (without surface coatings) show significant improvement in fretting fatigue strength [8].

Reference [9] found that surface treatments like Laser Shock Processing (LSP) and Low Plastic Burnishing (LPB) induce compressive residual stresses that can increase the fretting fatigue strength of the specimen by reducing the coefficient of friction but do not eliminate crack nucleation and propagation.

Reference [10] investigated the effect of Laser Shock peening on fretting fatigue life of Ti-6Al-4V specimens by applying the conditions similar to those as in blade/disc contacts in gas turbine. As compare to untreated specimens the LSP specimen showed 5-, 10-, 15-fold increase in fretting lives although it cannot eliminate the formation of fretting fatigue cracks and the fretting cracks were distributed throughout the surface.

Highly localized contact stresses were found to be responsible for crack nucleation. Sum of initiation life (using Socie paremeter, Chu-Bonnen parameter, Findley parameter and σ_{eq}) and propagation life gave the total predicted life. Shot peening increased the stresses at which run out (10^6 cycles) occur from 170 to 275 MPa. Coated specimens after losing their coating in first 50,000 cycles seen to have same failure life as of the shot peened specimen. Fig. 5. exhibits the methodology adopted in this study [11].

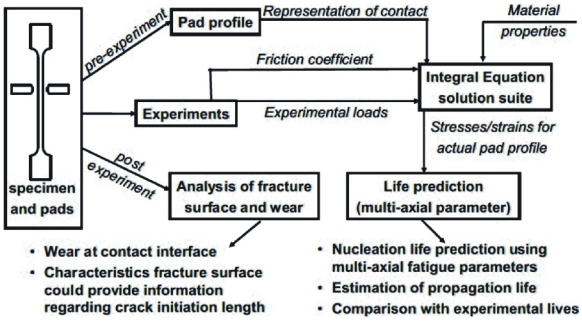

Fig. 5. Methodology adopted to study fretting fatigue phenomenon. [11]

Selected surface treatment techniques: diffusion treatments, hard coatings (TiN and CrN), soft coating (Cu-Ni-In), titanium-matrix TiB_2 in situ formed composite and shot peening were used to evaluate which one is best to enhance the tribological performance of Ti-6Al-4V and 60Ni-40Ti. They found that surface treatments significantly improve the wear performance of the specimens but their relative rankings varied significantly with lubricated and non-lubricated conditions [12]. CrN coated specimen exhibited least amount of wear as shown in Fig. 6.

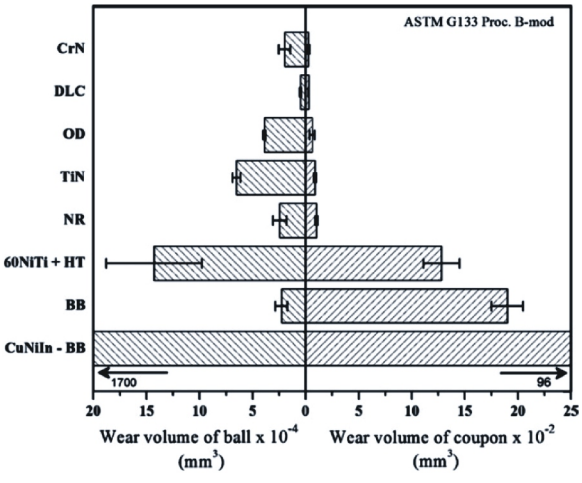

Fig. 6. Wear volume of coupons and balls tested under ASTM G133 Proc. B-mod. [12]

Reference [13] proposed a sequential finite element model (implicit and explicit) to study the effect of shot peening on shear stress, normal stress, bulk stress and slip amplitude which are key factors in fretting fatigue. Further it was found that compressive residual stresses had the major effect on fretting parameters and the mainly affected parameter was bulk stress.

Reference [14] used the technique of Ultrasonic

Non-crystalline Surface Modification (UNSM) and conducted lubricated fretting wear and friction tests using ball-on-flat specimen configuration of commercially available pure titanium and Ti-6Al-4V. Fretting wear debris of UNSM-treated specimens was found to be smaller and shallower than the untreated specimens. Also grain size was refined from 35.5µm to 200nm. Surface hardness also showed increment.

Reference [15] studied the electrochemical behavior of chromium nano-carbide coating applied using HVOF thermal spray technique under atmospheric conditions up to a finished thickness of 100µm on Ti-6Al-4V and Co-Cr-Mo alloys. All coated material showed greater corrosion resistance to mechanical abrasion as compare to native alloys. The presence of H_2O_2 at high temperature and low pH causes reduction in corrosion resistance of all the materials.

X-ray photoelectron spectroscopy and SEM with energy dispersive X-ray microanalysis was employed to study the effect of mechanical treatment on the surface chemical state, composition and morphology of commercially available Ti-6Al-4V. A considerable grain refinement along with the formation of nitrides and oxynitrides (both within and outside the contact area) was observed by ultrasonic impact treatment of Ti-6Al-4V in the presence of liquid nitrogen environment. The highest microhardness was found of the sample undergone ultrasonic impact treatment for 120s. For the first time mechano-chemical synthesis of nitrides in the Ti-6Al-4V alloys was found to occur at a high rate under ultrasonic impact in liquid nitrogen environment at cryogenic temperature [16].

Reference [17] investigated the wear and corrosion response of electroplated Ni/CNT composite coating on Ti-6Al-4V in Hank's solution and experimentally observed that the presence of CNT in the coating increases hardness of the alloy up to 98.5% higher than that of pure Ni coating. Moreover, this coating forms a stable and dense passive coating that improves wear and corrosion resistance in Hank's solution.

2.2 Crack Growth

A crack may be defined as the displacement discontinuity in a solid material due to applied stress. Prediction of crack growth is the primary objective of damage tolerance discipline.

10% of total life and 100% of life tests were conducted involving the application of fretting fatigue cycles followed by characterization of fretting damage using SEM and surface roughness measurement, marking of fretting cracks by using heat tinting and then the fracture of all the specimens under uniaxial loading. Fig. 7. shows residual fatigue strength results for 10% and 100% of total life. Cracks were nucleated near the edges and stress or strain criterion was found to be the predominating criteria causing nucleation of cracks. Cracks nucleated having surface lengths of 100µm or less have no effect on the fatigue strength. No correlation was found between surface roughness and fretting damage [18].

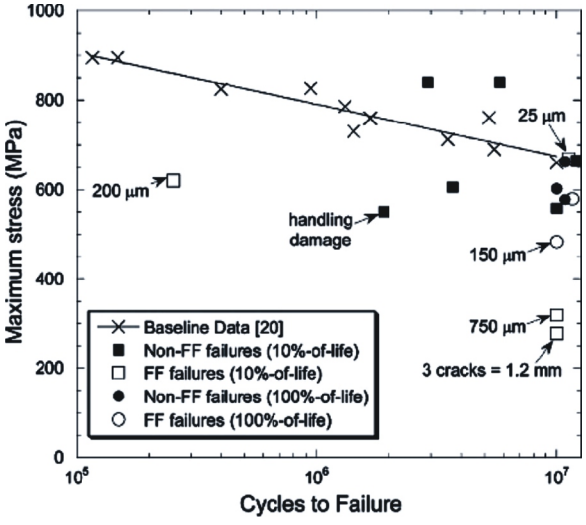

Fig. 7. Residual fatigue strength. [18]

C-shaped Ti-6Al-4V pads were utilized as test specimens which were previously used in fretting fatigue tests and heat tinting to locate the cracks and heat treated to release the stresses. High cycle fatigue step testing was conducted and threshold stresses were calculated while crack propagation threshold ΔK_{th} was calculated form measure crack sizes. When specimen failed at the leading edge the depth of damaging crack was found to be 75µm and 50µm when failed from the trailing edge [19].

Ti-6Al-4V dovetail specimen were tested using tension-compression MTS with an aim to establish a quantitative description of its fretting response under ambient conditions. An energy approach was used to formulated frictional behavior under gross slip conditions and a normalized wear parameter was derived that quantified the wear kinetics of Ti-6Al-4V irrespective of pressure, relative sliding amplitude, duration or contact dimensions [20]. Fig. 8 shows debris flow chart for the wear kinetics of titanium specimen.

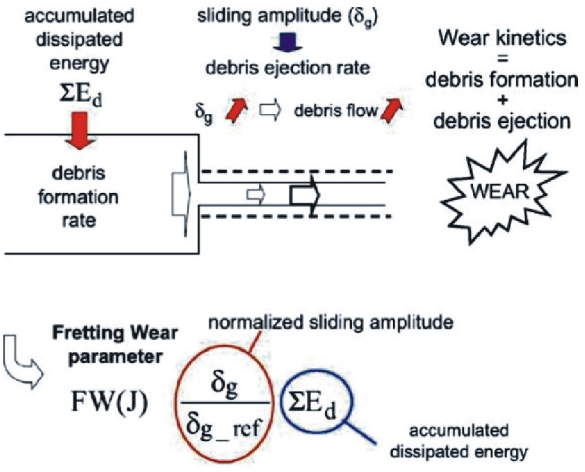

Fig. 8. Debris flow chart illustrating the Ti-6Al-4V wear kinetics at gross slip conditions. [20]

Influence of variation in microstructure of α/β Ti-6Al-4V was investigated which varied from homogenous duplex to fully transformed heterogeneous lamellar structure on fretting crack initiation. With this change in microstructure, the resistance to fretting initiated crack was found to be decreasing. Also it was observed that crack growth rate decrease consistently with the increase in the colony size at a certain given stress intensity factor [21]. Fig. 9 shows the S-N relationships for the three microstructures.

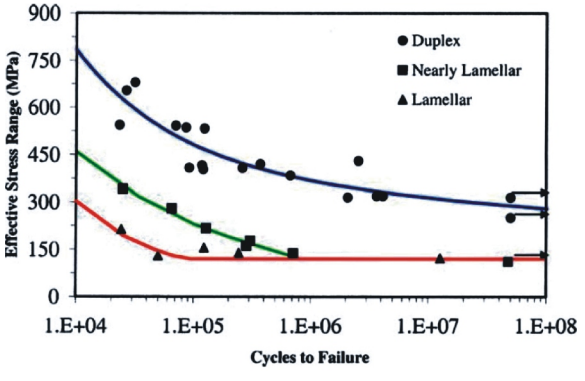

Fig. 9. S-N relationship based upon effective stress for three microstructures. [21]

Reference [22] analyzed the fractured surfaces of Ti-6Al-4V dog-bone and C-shaped specimens obtained after fretting fatigue tests on four point bending machine using optical and SEM. Fretting cracks were found to be small and shallow in depth and are concentrated/present around contacting interface perimeter and propagate into the material on elliptical fronts depending on stress gradient, geometry of contact and material properties. Fig. 10 shows SEM fractograph of C-specimen.

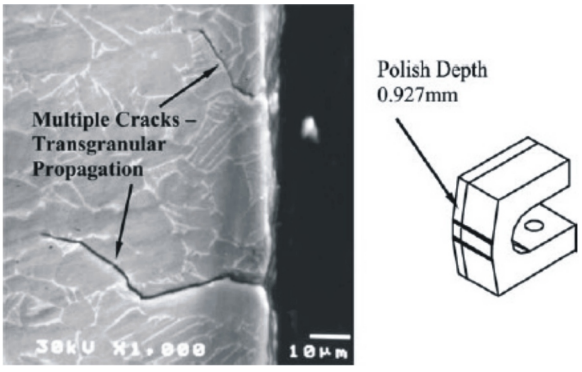

Fig. 10. Fretting crack profile produced on the C-specimen. [22]

Reference [23] investigated the fretting nucleated crack propagation unique double dogbone Ti-6Al-4V specimen under two conditions: high clamping stress and low clamping stress. Fractured surfaces were subjected to careful fractographic investigation and crack lengths were measured using SEM while AFGROW was utilized for crack propagation analysis. Fretting fatigue cycles were found to have no effect on the residual strength of the material until the crack depth exceeds 50μm. A high coefficient of friction was found to be responsible for the experimentally obtained crack propagation lives.

Fretting fatigue crack growth behavior in Ti-6Al-4V specimens with two types of contact geometries: cylindrical pads with 50.8 mm radius and flat pad with rounded edges was investigated using fracture mechanics based analysis technique and finite element sub-modeling using ABAQUS (for the specimen analysis when no crack is formed) and FRANC2D/L (for crack propagation). Effects of contact load, maximum tangential force and coefficient of friction on crack propagation life were studied. Under high cycle fatigue regime, crack nucleation and initiated consumes greater than 90% of total fretting fatigue life. As the initial crack length increases the grain size by two or three times, dependency of normalized crack propagation life on initial crack length vanishes [24].

Reference [25] presented and validated a model that quantifies the effect of fretting wear upon fretting crack initiation. The fretting fatigue tests were conducted at room temperature using cylinder-on-flat configuration showing dependence of crack behavior on slip regime and fretting scars were studied using profilometry and SEM. To model the cyclic plastic behavior of Ti-6Al-4V a linear kinematic hardening plasticity model was introduced. Spatial adjustment for the contact nodes in the simulation was achieved by user subroutine UNMESHMOTION together with an adaptive meshing framework with in ABAQUS.

Reference [26] studied the effect of stress gradient on the crack nucleation of cylinder/plane Ti-6Al-4V specimen under low cycle fatigue conditions. Plain

fatigue experiments were conducted using MTS hydraulic machine. Cracking zone in dovetail joint has been illustrated in Fig. 11. Crossland and Papadopoulos fatigue criterions were examined and compared. The results of three non-local approaches allowed the proper prediction of the threshold with in margin of error 3-5%. Square averaging, critical distance and weighted function approaches were also been employed and compared.

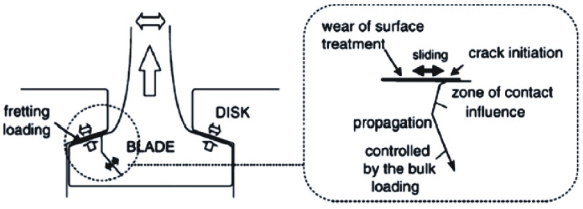

Fig. 11. The fretting fatigue crack found in dovetail joints of turbine engines. [26]

A micro-mechanical modeling methodology for fretting fatigue crack prediction in Ti-6Al-4V was presented based upon unit cell crystal plasticity model, frictional contact model and implementation of a microstructure sensitive fatigue indication parameter for indication of crack nucleation. A cylinder-on-flat configuration was employed. The microstructure-sensitive approach predicted partial slip cracking, corresponding with experimental data and was adopted to facilitate a novel wear prediction methodology [27].

2.3 Heat Treatment

The main purpose of heat treatment is to acquire desired physical, chemical and mechanical properties in a specimen. Heat treatment includes: annealing, case hardening, precipitation strengthening, quenching and tempering.

Reference [28] studied the relaxation behavior of residual stress in dogbone Ti-6Al-4V specimens (un-peened and shot-peened) during fretting fatigue tests at room temperature, 100 and 260^{0}C while stress ranging from 333 to 666MPa. Greater residual stress relaxation was found to occur when high cyclic load, contact load and temperature are increased. Comparison and analysis of stress relaxation behavior and corresponding fretting fatigue lives was carried out at different testing conditions. Fig. 12 shows the effect of temperature and time on stress relaxation.

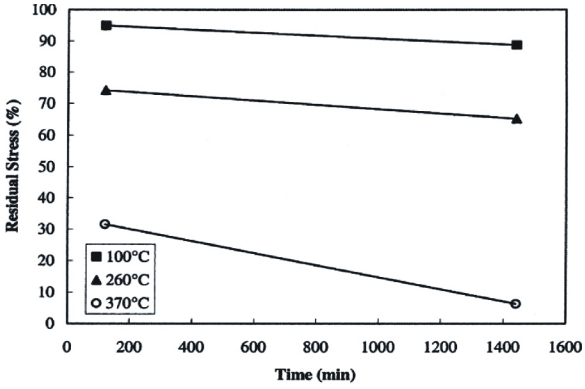

Fig. 12. Graph showing temperature effect and exposure time effect on residual stress relaxation. [28]

Fretting fatigue lives of Ti-6Al-4V flat-on-cylinder configuration specimen and pads were observed by conducting the experiments and through finite element analysis by using ABAQUS both at room temperature and at 260^{0}C. Specimens were subjected to a number of heat treatment processes: solution heat treatment at 935^{0}C and annealing at 700^{0}C. The coefficient of friction and its variation was found similar at both temperatures due to the fact that glaze oxide layer does not form on specimens' surface at 260^{0}C. Moreover, no difference in data values for plain fatigue and fretting fatigue lives were found at room temperature and at 260^{0}C [29].

Effect of cutting speed on fatigue lives of alpha-beta Ti-6Al-4V (ASTM Grade 5 and Grade 23) specimens was studied which were mill annealed and beta annealed. The surface roughness of all the materials was between 0.29μm and 0.44μm. Stress level was 600 MPa. It was found that cutting speed within the range of 50-150 m/min had no measureable influence on fatigue lives of either of the alloys and mill annealed heat treated specimens had greater fatigue lives than beta annealed heat treated specimens [30]. Fatigue life at various cutting speeds and surface conditions is shown in Fig. 13.

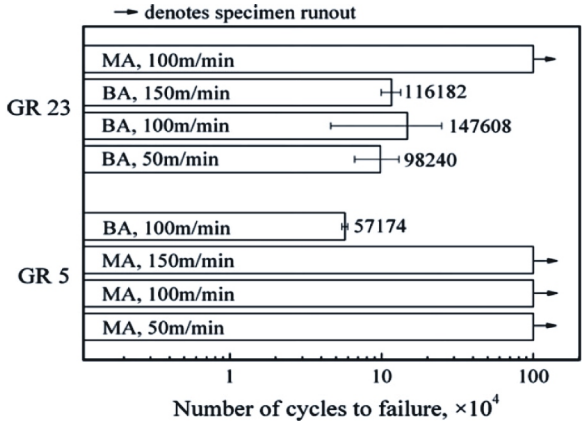

Fig. 13. Mean fatigue life of different materials at various cutting speeds. [30]

Effect of plasma nitriding under a gas mixture of $N_2/H_2 = 4$ at temperature varying from 700 to 850^{0}C for time durations from 2 to 10h was studied on tribological characteristics of Ti-6Al-4V disc shaped specimens. Plasma nitriding system is shown in Fig. 14. An increase in surface hardness, surface roughness, wear resistance, dynamic load-ability and coefficient of friction was observed due to plasma nitriding at increasing temperature and time. SEM, AFM, XRD and micro hardness techniques were employed for surface characteristic evaluation [31].

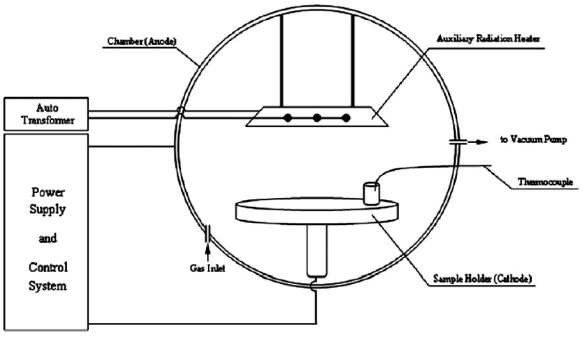

Fig. 14. Schematic diagram of plasma nitriding system used in this study [31]

2.4 Types of Loading

The damage caused by fretting fatigue depends a lot upon the type and load amplitudes.

Fretting fatigue response of Ti-6Al-4V dogbone specimens under varying and constant amplitude loadings at room temperature was investigated using servo-hydraulic uniaxial load frame. At higher frequencies fretting fatigue lives were found to be less than those found at low frequencies. For the predictions of variable amplitude loading tests Miner's linear summation model was applied. Microscopic examination revealed fretting surfaces for variable amplitude similar to those at 200Hz constant amplitude [32]. Fig. 15. shows the test rig.

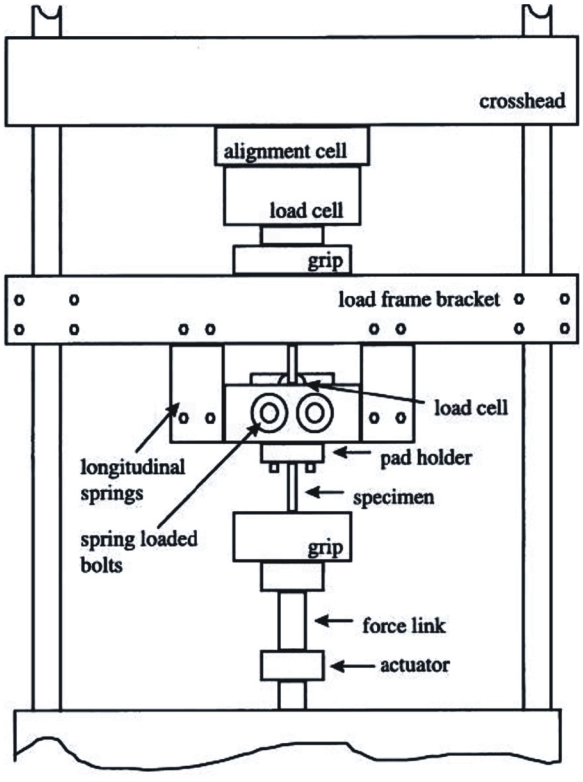

Fig. 15. Schematic diagram of fretting fatigue test frame [32]

Reference [33] investigated the fretting fatigue response of Ti-6Al-4V specimens and pads of flat-on-cylinder configuration using servo-hydraulic fatigue testing machine under variable loading conditions which involved two frequencies: 1Hz and 200Hz. The experimental fretting fatigue data differed from the predicted data obtained from Palmgren-Miner linear damage rule and hence it was found that in this case of variable amplitude loading condition, linear method of damage accumulation is less suitable than nonlinear method to estimate the fretting fatigue strength.

An investigation was carried out to establish a baseline for dry fretting contacts and to characterize the fretting response of Ti-6Al-4V on Ti-6Al-4V in point contact at high pressure. The material response and running condition at room temperature and 260^{0}C was same [34].

Reference [35] conducted a strain controlled multiaxial fatigue tests at room temperature on tubular Ti-6Al-4V specimens. Two types of proportional loadings (push-pull and reversed torsion) and two non-proportional (900 phase difference) loadings were applied. There was considerable decrease in fretting fatigue lives due to non-proportional loading about 1/10th than that for proportional loading for the same amplitude of strain via Mises' equivalent model. Fig. 16 shows Mises' equivalent stress-strain relationship.

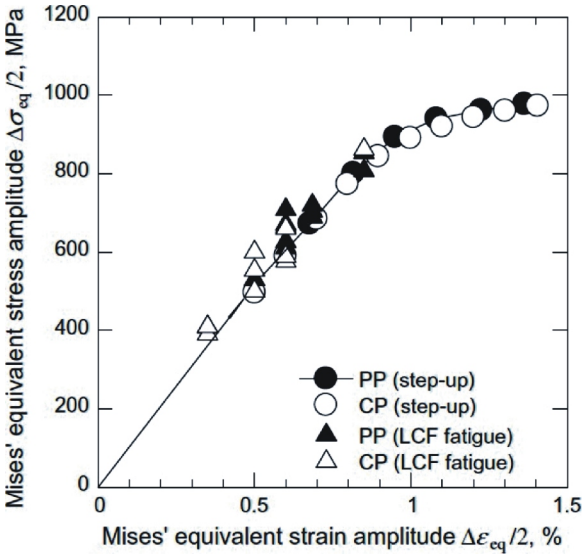

Fig. 16. Cyclic stress-strain relations. [35]

2.5 Contact Pads

Contact pads are subjected to high level of contact stresses that can also initiate cracks in them. Contact pad geometry and material are of prime importance in fretting fatigue tests.

Fretting fatigue tests using Ti-6Al-4V cylindrical and flat pads with rounded edges and at different pad displacements with two normal forces on the pad were conducted. These tests were performed at stress range amplitude 266MPa. Fretting fatigue life was found to be minimum and independent of the contact configuration at relative slip range between 50µm and 60µm. Tangential force and tangential to normal force ratio increased in direct relation with pad displacement independent of its geometrical shape. Contact configuration affected the fretted surface profile [36].

Reference [37] developed a setup to study the fretting fatigue response of Ti-6Al-4V dog-bone specimen capable of applying independent pad displacement (measured using extensometer) under normal force and stress amplitude conditions. Fretting fatigue life was minimum at slip ranges between 50µm and 60µm but increases as the relative slip increases and above 60µm the specimen does not fail due to gross sliding.

Effect of dissimilar mating materials on the fretting fatigue response of Ti-6Al-4V flat specimen was studied which was initially tested on uniaxial hydraulic machine against cylindrical pads made of Ti-6Al-4V, aluminum alloy 2024 and Inconel 718. Finite element analysis was performed using ABAQUS. At the same level of applied stress, there was no significant difference found in the fretting fatigue lives by using different pad materials. Later prediction of number of cycles for crack initiation was done by using modified SWT, SSR, MSSR and Findley parameter while only SSR and MSSR parameters were found to predict the location and orientation of the crack initiation precisely [38].

Reference [39] investigated Ti-6Al-4V specimen in contact with the pads of two different materials (aluminum 2024 and Inconel 718) at different levels of applied stresses and contact forces. Finite element analysis showed that increase in amount of the contact force results in smaller relative slip and greater width of stick zone. In general, the specimens which were fretted at lower contact force showed more damage on the contact surface than those subjected to high contact force.

Reference [40] investigated the mechanical and microstructural response of fretted Ti-6Al-4V specimen and pads. Fretting frequency was 100Hz and these tests were conducted using MTS 810. Three types of fretting pads were used: one with 3mm flat dimension with chamfered edges, second 1 mm chamfered edge and third with 3mm flat and 3mm transition radius as shown in Fig. 17. Pad geometry was found to have no effect on the fretting generated cracks.

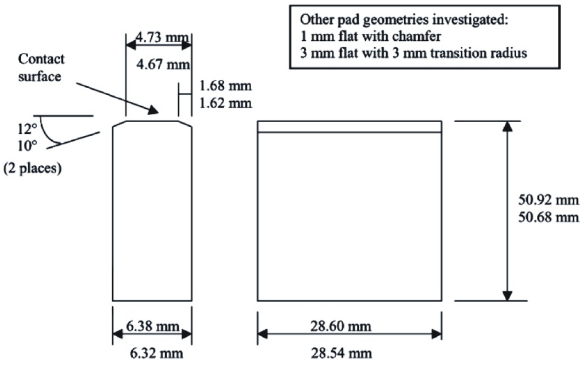

Fig. 17. Fretting pad geometry. [40]

2.6 Life Prediction Models

A series of remote fatigue tests on Ti-6Al-4V C-shaped specimen were conducted that were previously undergone to fretting fatigue loading conditions. CAFDEM was used to analyze the contact stresses developed in the tested specimen. Equivalent stress model provided a reasonable approach for correlation of total specimen life tested at wide range of loadings. MATLAB code was utilized for the calculation of fatigue crack propagation life [41].

A fretting life prediction model was applied for Ti-6Al-4V dog-bone shape specimens. The life prediction model included crack initiation life and crack propagation life along with initial flaw size determination. This model was applied to two types of fretting fatigue experiments and also compared with existing life prediction models. CAPRI was used for the stress determination. This model successfully predicts the experimental data and proves to be a good achievement [42]. Fig. 18. shows stress profile into depth of specimen considering opening and closing of crack.

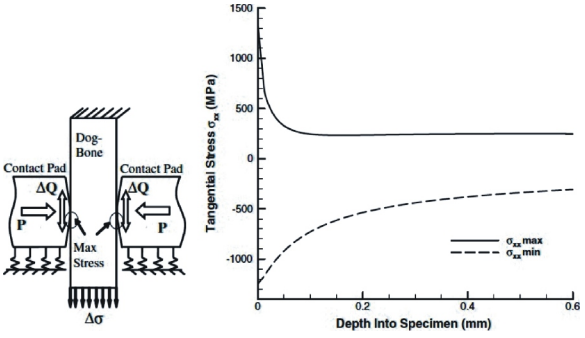

Fig. 18. Figure showing tangential stress profiles into the depth of specimen considering opening and closing of cracks. [42]

A new probabilistic analysis was developed to predict the fretting fatigue lives of Ti-6Al-4V specimens by considering the effects following variables: initial crack size, coefficient of friction, relative slip, contact pad profile and crack growth law. Various quantitative and qualitative techniques were applied to the results including probabilistic sensitivities via linear regression. Monte Carlo sampling was used as input in this study [43].

III. Conclusions

Findings of fretting fatigue behavior of Ti-6Al-4V by considering the effects of various surface treatments, crack growth, heat treatment processes, types of loadings, contact pad configurations and life prediction models can be summarized to get to the following conclusions:

1. Surface treatment processes like shot peening (SP), ion-beam-enhanced deposition (IBED) CrN films, (SP) + IBED CrN films, Laser Shock Processing and Diamond Like Carbon (DLC) coated specimens increased their fretting fatigue strength by inducing compressive residual stress, reducing coefficient of friction, increasing surface roughness and hardness. Furthermore it was found that re-shot peening can eliminate the effects of any damage occurred after initial shot peening due to fretting phenomenon.
2. Cracks were nucleated near the edges and stress or strain criterion was found to be the predominating criteria causing nucleation of cracks. Cracks are small and shallow in depth and concentrate around the contacting interface perimeter and propagate into the material depending upon stress gradient, geometry and material properties. More than 90% of total fatigue life was consumed during nucleation and initiation of cracks under high cycle fatigue.
3. Greater residual stress relaxation was found to occur when high cyclic load, contact load and temperature were increased. Moreover, mill annealed heat treated specimens had greater fatigue lives than beta annealed heat treated specimens. Plasma nitriding causes surface increase in surface hardness, toughness, wear resistance, dynamic load-ability and coefficient of friction at increasing temperature and time.
4. Microscopic examination revealed fretting surfaces for variable amplitude loadings similar to those at 200Hz constant amplitude loadings. In case of variable amplitude loading linear method of damage accumulation was found to be less appropriate than nonlinear method for estimating fretting fatigue life. There was considerable decrease in fretting fatigue lives due to non-proportional loading about 1/10th than that for proportional loading for the same amplitude of strain using Von Mises' equivalent model.
5. At the same level of applied stress, there was no significant difference observed in the fretting fatigue lives by using different pad materials. Also it was found that fretting pad geometry had no effect on the cracks generation.

References

[1] V. A. Joshi, "Titanium Alloys: An Atlas of Structures and Fracture Features," CRC Press, 2006.

[2] *Materials Properties Handbook: Titanium Alloys,* eds. ASM, R. Boyer, G. Welsch, E. W. Collings, eds. ASM International, Materials Park, OH, 1994.

[3] Y. Fu, N. L. Loh, A. W. Batchelor, D. Liu, X. Zhu, J. He, K. Xu. (1998). Improvement in fretting wear and fatigue resistance of Ti6Al4V by application of several surface treatments and coatings. *Surface and Coatings Technology, 106,* 193-197.Available: http://www.sciencedirect.com/science/article/pii/S0257897298005283

[4] A. L. Hutson, M. Niinomi, T. Nicholas, D. Eylon. (2002). Effect of various surface conditions on fretting fatigue behavior of Ti6Al4V. *International Journal of Fatigue, 24*, 1223-1234. Available: http://www.sciencedirect.com/science/article/pii/S0142112302000506

[5] H. Lee, S. Mall, S. Sathish (2005). Investigation into effects of re-shot-peening on fretting fatigue behavior of Ti6Al4V. *Materials Science and Engineering, A 390*, 227-232. Available: http://www.sciencedirect.Com/science/article/pii/S0921509304010755

[6] W. Ren, S. Mall, J. H. Sanders, S. K. Sharma (2005). Evaluation of coatings on Ti6Al4V substrate under fretting fatigue. *Surface & Coatings Technology, 192,* 177-188. Available: http://www.sciencedirect.com/science/article/pii/S0257897204006097

[7] H. Lee, S. Mall. (2006). Fretting behavior of shot peened Ti6Al4V under slip controlled mode. *Wear, 260*, 642-651. Available: http://www.sciencedirect.com/science/article/pii/S0043164805002905

[8] P. J. Golden, A. Hutson, V. Sundaram, J. H. Arps. (2007). Effect of surface treatments on fretting fatigue of Ti6Al4V. *International Journal of Fatigue, 29*, 1302-1310. Available: http://www.sciencedirect.com/science/article/pii/S0142112306003008

[9] P. J. Golden, M. J. Shepard (2007). Life prediction of fretting fatigue with advanced surface treatments. *Materials Science and Engineering, A 468-470*, 1522. Available: http://www.sciencedirect.com/science/article/pii/S0921509307002961

[10] S. Srinivasan, D. B.Garcia, M.C.Gean, H.Murthy, T. N. Farris (2009). Fretting fatigue of laser shock peened Ti6Al4V. *Tribology International 42*, 1324-1329. Available: http://www.sciencedirect.Com/science/article/pii/S0301679X09000917

[11] H. Murthy, G. Mseis, T. N. Farris (2009). Life estimation of Ti6Al4V specimens subjected to fretting fatigue and effect of surface treatments. *Tribology International, 42*,1304-1315. Available: http://www.sciencedirect.com/science/article/pii/S0301679X09000899

[12] D. G. Bansal, O. L. Eryilmaz, P. J. Blau (2011). Surface engineering to improve the durability and lubricity of Ti6Al4V alloy. *Wear, 271*, 2006-2015. Available: http://www.sciencedirect.com/science/article/pii/S0043164811001098

[13] S. M. H-Gangaraj, Y.Alvandi-Tabrizi, G. H. Farrahi, G. H. Majzoobi, H. Ghadbeigi. (2011). Finite element analysis of shot-peening effect on fretting fatigue parameters. *Tribology International, 44*, 1583-1588. Available: http://www.sciencedirect.Com/science/article/pii/S0301679X10003129

[14] A. Amanov, I. Cho, D. Kim, Y. Pyun. (2012). Fretting wear and friction reduction of CP titanium and Ti6Al4V alloy by ultrasonic nanocrystalline surface modification. *Surface & Coatings Technology, 207*, 135-142. Available: http://www.sciencedirect.Com/science/article/pii/S0257897212006159

[15] V. Swaminathan, H. Zeng, D. Lawrynowicz, Z. Zhang, J. L. Gilbert. (2012). Electrochemical investigation of chromium nanocarbide coated Ti6Al4V and CoCrMo alloy substrates. *Electrochimica Acta, 59*, 387-397. Available: http://www.sciencedirect.com/science/article/pii/S0013468611016379

[16] M. A. Vasylyev, S. P. Chenakin, L. F. Yatsenko. (2012). Nitridation of Ti-6Al-4V alloy under ultrasonic impact treatment in liquid nitrogen. *Acta Materialia, 60,* 6223-6233. Available: http://www.sciencedirect.com/science/article/pii/S1359645412005356

[17] C.K. Lee. (2012). Wear and corrosion behavior of electrodeposited nickelcarbon nanotube composite coatings on Ti6Al4V alloy in Hanks' solution. *Tribology International, 55*, 714. Available:http://www.sciencedirect.com/science/article/pii/S0301679X12001867

[18] A. L. Hutson, C. Neslen, T. Nicholas. (2003). Characterization of fretting fatigue crack initiation processes in CR Ti6Al4V. *Tribology International, 36,* 133-143. Available:http://www.sciencedirect.com/science/article/pii/S0301679X0200138X

[19] P. J. Golden, B. B. Bartha, A. F. Grandt Jr., T. Nicholas. (2004). Measurement of the fatigue crack propagation threshold of fretting induced cracks in Ti6Al4V. *International Journal of Fatigue, 26,* 281-288. Available: http://www.sciencedirect.com/science/article/pii/S014211230300166X

[20] S. Fouvry, P. Duó, Ph. Perruchaut. (2004). A quantitative approach of Ti6Al4V fretting damage: friction, wear and crack nucleation. *Wear, 257*, 916-929. Available:Http://www.sciencedirect.com/science/article/pii/S0043164804001218

[21] S. Mall, S. A. Namjoshi, W. J. Porter. (2004). Effects of microstructure on fretting fatigue crack initiation behavior of Ti-6Al-4V. *Materials Science and Engineering, A 383*, 334-340. Available:http://www.sciencedirect.com/science/article/pii/S0921509304005416

[22] D. B. Garcia, A. F. Grandt Jr. (2005). Fractographic investigation of fretting fatigue cracks in Ti6Al4V. *Engineering Failure Analysis, 12*, 537-548. Available: http://www.sciencedirect.com/science/article/pii/S135063070400127X

[23] A. Hutson, T. Nicholas, R. John. (2005). Fretting fatigue crack analysis in Ti6Al4V. *International Journal of Fatigue, 27*, 1582-1589. Available: http://www.sciencedirect.com/science/article/pii/S0142112305001787

[24] H. A. Fadag, S. Mall, V. K. Jain. (2008). A finite element analysis of fretting fatigue crack growth behavior in Ti6Al4V. *Engineering Fracture Mechanics, 75,* 1384-1399. Available: http://www.sciencedirect.com/science/article/pii/S0013794407002925

[25] J. Ding, G. Bandak, S. B. Leen, E. J. Williams, P. H. Shipway. (2009). Experimental characterization and numerical simulation of contact evolution effect on fretting crack nucleation for Ti6Al4V. *Tribology International, 42*, 1651-1662. Available: http://www.sciencedirect.com/science/article/pii/S0301679X09001212

[26] R. Ferré, S. Fouvry, B. Berthel, J. A. Ruiz-Sabariego. (2013). Stress gradient effect on the crack nucleation process of a Ti6Al4V titanium alloy under fretting loading: Comparison between non-local fatigue approaches. *International Journal of Fatigue, 54*, 56-67. Available: http://www.sciencedirect.com/science/article/pii/S0142112313000844

[27] O. J. McCarthy, J. P. McGarry, S. B. Leen. (2013). Micro-mechanical modelling of fretting fatigue crack initiation and wear in Ti6Al4V. *International Journal of Fatigue xxx,* xxxxxx. Available: http://www.sciencedirect.com/science/article/pii/S0142112313001254

[28] H. Lee, S. Mall. (2004). Stress relaxation behavior of shot-peened Ti6Al4V under fretting fatigue at elevated temperature. *Materials Science and Engineering, A366,* 412-420. Available: http://www.sciencedirect.com/science/Article/pii/S0921509303009602

[29] O. Jin, S. Mall, O. Sahan. (2005). Fretting fatigue behavior of Ti6Al4V at elevated temperature. *International Journal of Fatigue, 27*, 395-401. Available:http://www.sciencedirect.com/science/article/pii/S0142112304001793

[30] W. Niu, M. J. Bermingham, P. S. Baburamani, S. Palanisamy, M.S. Dargusch, S. Turk, B. Grigson, P. K. Sharp. (2013). The effect of cutting speed and heat treatment on the fatigue life of Grade 5 and Grade 23 Ti6Al4V alloys. *Materials and Design, 46,* 640-644. Available:http://www.sciencedirect.com/science/article/pii/S0261306912007546

[31] S. R. Hosseini, A. Ahmadi. (2013). Evaluation of the effects of plasma nitriding temperature and time on the characterisation of Ti 6Al 4V alloy. *Vacuum, 87*, 30-39. Available: http://www.sciencedirect.com/science/article/pii/S0042207X12003314

[32] R. Cortez, S. Mall, J. R. Calcaterra. (1999). Investigation of variable amplitude loading on fretting fatigue behavior of Ti6AlV. *International Journal of Fatigue, 21*, 709-717. Available: http://www.sciencedirect.com/Science/article/pii/S0142112399000341

[33] S. A. Namjoshi, S. Mall. (2001). Fretting behavior of Ti-6Al-4V under combined high cycle and low cycle fatigue loading. *International Journal of Fatigue, 23*, S455-S461. Available: http://www.sciencedirect.com/science/article/pii/S0142112301001438

[34] X. Huang, R.W. Neu. (2008). High-load fretting of Ti6Al4V interfaces in point contact. *Wear, 265,* 971-978.Avaialble: http://www.sciencedirect.com/science/article/pii/S0043164808000756

[35] M. Wu, T. Itoh, Y. Shimizu, H. Nakamura, M. Takanashi. (2012). Low cycle fatigue life of Ti6Al4V alloy under non-proportional loading. *International Journal of Fatigue, 44*, 1420. Available:http://www.sciencedirect.com/science/article/pii/S0142112312002071

[36] O. Jin, S. Mall. (2002). Influence of contact configuration on fretting fatigue behavior of Ti6Al4V under independent pad displacement condition. *International Journal of Fatigue, 24*, 1243-1253. Available:http://www.sciencedirect.com /science/article/pii/S0142112302000415

[37] O. Jin, S. Mall. (2002). Effects of independent pad displacement on fretting fatigue behavior of Ti6Al4V. *Wear, 253*, 585-596. Available: http://www.sciencedirect.com/science/article/pii/S0043164802000613

[38] H. Lee, O. Jin, S. Mall. (2004). Fretting fatigue behavior of Ti6Al4V with dissimilar mating materials. *International Journal of Fatigue, 26,* 393-402. Available: Http://www.sciencedirect.com/science/article/pii/S0142112303001968

[39] H. Lee, S. Mall. (2004). Effect of dissimilar mating materials and contact force on fretting fatigue behavior of Ti6Al4V. *Tribology International, 37,* 35-44. Available: http://www.sciencedirect.com/science/article/pii/S0301679X03001129

[40] W. A. Glaeser, B. H. Lawless. (2001). Behavior of alloy Ti6Al4V under pre-fretting and subsequent fatigue conditions. *Wear, 250*, 621-630. Available: http://www.sciencedirect.com/science/article/pii/S004316480100669X

[41] P. J. Golden, A. F. Grandt Jr. (2004). Fracture mechanics based fretting fatigue life predictions in Ti6Al4V. *Engineering Fracture Mechanics, 71*, 2229-2243. Available: http://www.sciencedirect.com/science/article/pii/S0013794404000049

[42] D. B. Garcia, A. F. Grandt. (2007). Application of a total life prediction model for fretting fatigue in Ti6Al4V. *International Journal of Fatigue, 29*, 1311-1318. Available:http://www.sciencedirect.com/science/article/pii/S014211230600301X

[43] P. J. Golden, H. R. Millwater, X. Yang. (2010). Probabilistic fretting fatigue life prediction of Ti6Al4V. *International Journal of Fatigue, 32*, 1937-1947. Available: http://www.sciencedirect.com/science/article/pii/S014211231000143X

Minimization of Intercellular Movements in Cellular Manufacturing System Using Genetic Algorithm

M. Imran[1], N. Iqbal[2], M. Jahanzaib[3]

[1,2]*Industrial Engineering Department UET Taxila, Pakistan*
[2]*Industrial Engineering Department UET Taxila, Pakistan*
[1]imran.ime13@gmail.com
[2]neelumiqbal@yahoo.com
[3]jahan.zaib@uettaxila.edu.pk

Abstract-Cell formation in cellular manufacturing is necessary to achieve desired productivity, efficiency and quality. Genetic algorithm so developed is applied in cellular manufacturing system to design cells. Cells are arranged according to certain criteria and are defined by objective function which is evaluated for chromosome in each population. Objective function is to minimize intercellular movements because it increase lead time, work in process, cost of material handling and fatigue of workers. Genetic algorithm is biological evolution and natural selection process which is alternatively used for solving complex optimization problems. A population consisting of ten chromosomes has been created randomly and objective function value is calculated for each chromosome. Using genetic operators ten generations have been created and objective function value of each chromosome calculated using MATLAB for each generation. In 10^{th} generation a chromosome with minimized objective function is achieved and encoded to design cells with minimum intercellular movements of parts. It has been learnt that about fifty percent intercellular movements have been reduced by Genetic algorithm.

Keywords-Cellular Manufacturing, Cross Over, Elitism, Genetic Algorithm, Mutation, Population, cell formation

I. INTRODUCTION

Group technology has wide applications, and it has become popular in shop floor layout design. The operational benefits of flow line production can be achieved by using Cellular Manufacturing (CM) System. A group of parts, which are similar in some properties, are brought on a machine group in cellular manufacturing system to perform various operations. CM provides excellent results in the courses of simulation, analytical, surveys and actual implementations. They are: Reduction of setup time, Condensed Lot sizes, Reduction in Work-in-process and finished goods inventories, Condensed Throughput time and Improvement in working flexibility. Cellular Manufacturing system consists of a group of machines forming different cells. These cells are specialized in producing a specific part family. Cellular manufacturing has also become popular where different machines are grouped into a cell which is specialized in producing part family. Part family can be defined in the way where some parts have similar shapes and sizes or have similar processes steps. In CM, the issue is development of an efficient cell. Many techniques have been described to cope with this issue. Three approaches are used for cell formation: (a) part-family grouping, in which part families are formed and then machines are grouped into cells; (b) grouping of machines, in which cells of machines are formed taking into account homogeneity in movements and parts are assigned to cells; (c) machine-part grouping, in which part families and machine cells are formed all together. In this paper, objective is minimization of inter-cellular movements of parts and the focus in our case is identification of parts or machines to be grouped into cell. The work has been carried out in Genetic Algorithm (GA), in which several generations are solved to achieve multiple objective function values and best chromosome with minimum objective function is encoded to get optimal solution. Mutation and cross over operators are used in GA and are responsible for next generation. In crossover, information is combined from two parents to new offspring or child. By using crossover operator, best genes are removed from many chromosomes and then recombining them into better offspring. In mutation, new offspring are generated by making random changes in existing generation. It adds diversity to the population and increase the likelihood that best fitness value of the chromosomes can be generated. By using GA both constraint and unconstraint problems can be solved and usually it is applied in complex system where no of machines and production is very high.

II. Literature Review

Manufacturing or production systems perform the conversion of raw materials into useful products or services .Effectiveness of any manufacturing system is dependent on quality, time and cost [1]. A cellular manufacturing system consists of different cells and each cell specializes in one type of task. Cells can be formed on the basis of objective function and objective may be the minimization of the sum of the machine constant and variable costs, inter- and intra-cell material handling, a reconfiguration costs and this objective was achieved using simulated annealing [2]. Multi objective scheduling criteria can be used in CMS to design cell which have minimum make span, intracellular movement, tardiness, and sequence-dependent setup costs, using heuristic techniques [3]. Multi objective scheduling criteria can be used in CMS to design cell which have minimum make span, intracellular movement, tardiness, and sequence-dependent setup costs, using heuristic techniques [4].The objective of cell formation may be the presence of alternate process routings, operation sequence, duplicate machines, machine capacity and lot splitting. A mixed integer non-linear program was used to solve cell design problems [5]. Genetic algorithm is also being used to design cells with dynamic conditions and it provides best solution in any complexity of dynamic situation [6]. A multiobjective dynamic cell formation is carried out using genetic to minimize machine cost, inter-cell material handling cost, and machine relocation cost [7].When local search heuristic approach is combined with genetic algorithm it provides best optimal solution to cellular manufacturing system problems [8]. Genetic algorithm is being used in cellular manufacturing system, and their objective was the minimizing the interaction among cells [9]. The local search algorithm when combined with genetic algorithm provides intensified and diversified way to solve complex problems of cellular manufacturing system [10]. Genetic algorithm is more efficient algorithm as compared to CRAFT and entropy based algorithm and provides solution of problems with minimum total cost [11].Genetic algorithm can handle multiple objective functions i.e. Material handling costs, aspect ratio, closeness and distance requests.[12]

III. Research Methodology

GA is revolutionary algorithm and based on theory of evolution in organisms. It is being used to solve optimization problems which cannot be solved using traditional approaches. Formation of cells and movements from intercellular minimization is resolved using GA. It has capability of producing multiple solutions of single or multiple objective functions while traditional methods of optimization can produce one solution and probability of best result is less. Step wise GA coding in Cellular Manufacturing system is given as follows:

1. Parts routing from one machine to another is defined. Routing of all parts in different station is identified and a part /machine matrix is developed. Number of machines is eight and number of parts to be routed is nine.
2. Objective function on which formation of cell is carried out is defined and the objective is to reduce total number of movements of different parts in the cells.
3. GA is implemented to solve the problem of cell design and while implementing GA initial criteria is set i.e. Elitism, mutation, crossover, generation gap, population size and number of generation.
4. Initially a random chromosome is generated which consists of gene and represents one machine. Total number of genes in chromosomes is eight and each gene represents a machine and number of machines under consideration is eight.
5. Each digit in a chromosome represents cell number and these have been assigned randomly with initial population of ten chromosomes generated. Each chromosome in population is randomly generated. Objective function value of chromosome is calculated in initial population using MATLAB.
6. Further generations have been generated using genetic operators i.e. crossover and mutation and ten generations produced and optimal solution of cell design is achieved
7. A chromosome with minimum objective function value is encoded to achieve a optimal cell design which showed minimum procedure of GA is summarized in Fig.1.

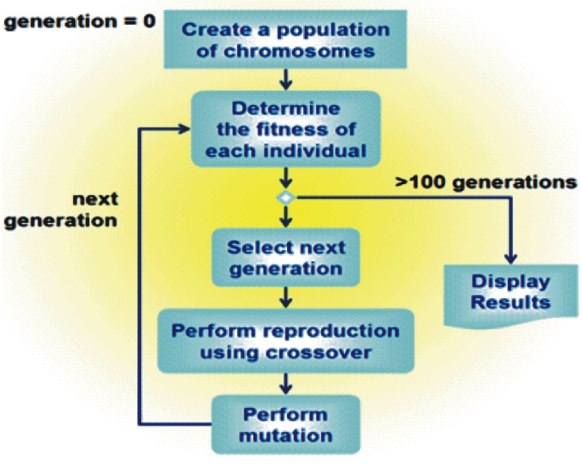

Fig. 1. Genetic Algorithm Process Flow

Data has been collected from shop floor. There were eight machines and manufacture nine different products. Currently machines are not properly installed at suitable locations in shop due to inappropriate layout of machines movements of work in process among different machines is very high which increases cost of manufacturing, fatigue of worker and cycle time of each process in job shop. This situation creates problems when demand of products is very high and shop is unable to meet the demand of products due to unnecessary movement among different machines. The sequence of movement of different parts in different machines is shown in Table I. as given below.

TABLE I
PARTS VISITATION MACHINES

PARTS	MACHINES							
	A	B	C	D	E	F	G	H
1	1						1	
2		1		1				
3			1		1			1
4				1			1	
5	1		1					1
6				1		1		
7		1		1		1		
8			1		1			
9	1			1			1	

Since nine parts are to be manufactured using eight machines and daily demand of each part is ten so daily production of workshop is 90 parts. Using the data from table 1 a part /machine matrix is created and it is shown in (1)

$$E_{ji} = \begin{bmatrix} 1 & 0 & 0 & 0 & 0 & 0 & 1 & 0 \\ 0 & 1 & 0 & 1 & 0 & 0 & 0 & 0 \\ 0 & 0 & 1 & 0 & 1 & 0 & 0 & 1 \\ 0 & 0 & 0 & 1 & 0 & 0 & 1 & 0 \\ 1 & 0 & 1 & 0 & 0 & 0 & 0 & 1 \\ 0 & 0 & 0 & 1 & 0 & 1 & 0 & 0 \\ 0 & 1 & 0 & 1 & 0 & 1 & 0 & 0 \\ 0 & 0 & 1 & 0 & 1 & 0 & 0 & 0 \\ 1 & 0 & 0 & 1 & 0 & 0 & 1 & 0 \end{bmatrix} \quad (1)$$

Matrix element zero '0' and one '1' shows the parts movements among different machines; if part visits the machine then it is represented by 1 other wise 0.

Eji is part machine matrix

where

j = part number
i = machine number

The objective function is the minimization of movements of parts among different machines and cell formation to achieve minimum inter-cellular movements. Objective function can be defined as;

Intercellular movements of parts
= (production requirment of each part)
× (no of movements of parts to each cell − 1)

Nj represents Production requirment of each part

Nj is matrix of form 1 × n

$$Xil = \begin{cases} 1 \text{ if machine "i" is in cell 1} \\ 0 \text{ if not in cell} \end{cases} \quad (2)$$

Eji is (n × m)matrix and Eji can be defined as

$$Eji = \begin{cases} 1 \text{ if part j is processed on M/c i} \\ 0 \text{ otherwise} \end{cases} \quad (3)$$

Machine is abbreviated with M/c in equation (3)

Yjl is a (part × cell matrix) and

$$Yjl = \begin{cases} 1 \; if \; \sum_{i=1}^{m} Eji \times Xil > 0 \; if \; part \; is \\ \text{processed in cell l} \\ 0 \text{ otherwise} \end{cases} \quad (4)$$

Actually Yjl shows movements of parts in cells. By combining all information about cells, machines and parts a mathematical objective function is created

$$F = \sum_{j=1}^{n} Nj\left[\sum_{l=1}^{k} Yjl - 1\right] \quad (5)$$

j = part number
i = machine number
n = total number of parts
m = total number of machines
k = total number of cells
Nj = demand of each part
yjl = parts × cell matrix [12]

3.1 Genetic Algorithm Procedure

When solving GA optimization problem for formation of cell in Cellular manufacturing system some initial parameters i.e. elitism criteria, mutation probability, cross over probability, generation gap, population size and number of generations are set. In this problems initial population size is ten so there are ten individuals (chromosomes) in each generation and

total number of generations are ten .Chromosomes with best fitness value are called elite chromosomes and elitism criteria for this problem is 20% i.e. if there are ten chromosomes then two chromosomes of all generation except parent generation which have minimum fitness function value are called elite children (chromosomes). Elite chromosomes remain unchanged in mutation and cross over in next generation. Cross over probability in this problem is 0.7 it means that out of eight chromosomes there are only six chromosomes on which cross over is to be performed and always a pair of chromosomes (Parents) participate in crossover. Mutation is another genetic operator which creates diversity in next generation and it always occurs in single chromosome. Mutation probability in this problem is 0.07 which means that there are only two chromosomes on which mutation takes place. Considering all parameters settings as explained can be further elaborated with the chromosome [2 1 3 2 3 1 1 2]. Since a chromosome consist of genes so in this chromosome there are eight genes and each gene represents machine. In above chromosome position of 1st digit represents 1st machine and position of 2nd digit represents 2nd machine and so on. Each digit in chromosome represents cell number; here we have assumed three cells , in case of above chromosome machines 6,7 and 2 are in cell 1 ; 1, 8 and 4 are in cell two ; 3 and 5 are in cell 3 as shown in Fig. 2.

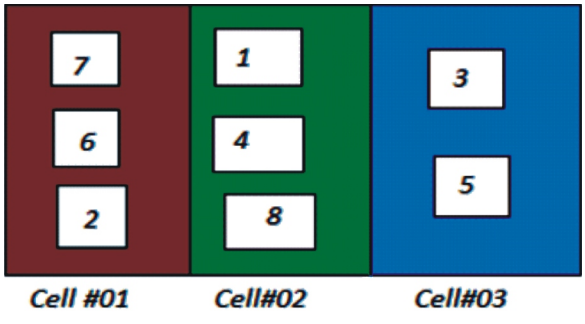

Fig. 2. Machines assigned in Cells

Calculation of Fitness Function Value

Using chromosme [2 1 3 2 3 1 1 2] a matrix which shows arrangement of different machines in different cells is created. It is represented by Xil and Xil is (machine × cell) matrix

$$X_{il}=\begin{bmatrix}0&1&0\\1&0&0\\0&0&1\\0&1&0\\0&0&1\\1&0&0\\1&0&0\\0&1&0\end{bmatrix} \quad (6)$$

Matrix (1) is a Parts × machine matrix; and

A = Eji × Xil

$$= \text{(Parts/Machine)} \times \text{(Machine/ cell)} \quad (7)$$

$$A=E_{ji} * Xil = \begin{bmatrix}1&1&0\\1&1&0\\0&1&2\\1&1&0\\2&1&0\\0&0&2\\1&2&0\end{bmatrix} \quad (8)$$

A = Eji × Xil =Parts/Cell Matrix; here A is matrix

Which shows the movements of parts in cells. Yjl is already defined above in (4). Now if part visits the cell then it is represented by 1 otherwise 0 so above (8) can be written as

$$Yjl = A>0Y_{jl}=\begin{bmatrix}1&1&0\\1&1&0\\0&1&1\\1&1&0\\0&1&1\\1&1&0\\1&1&0\\0&0&1\\1&1&0\end{bmatrix} \quad (9)$$

In order to calculate intercellular movement of parts transpose of Yjl is used which can be represented by B=Yjl' and Yjl' is transpose of Yjl.

$$B=Y_{jl}{}'=\begin{bmatrix}1&1&0&1&0&1&1&0&1\\1&1&1&1&1&1&1&0&1\\0&0&1&0&1&0&0&1&0\end{bmatrix} \quad (10)$$

(11) shows the intercellular movement of each part.

$$C = \text{sum}(B) = [2\ \ 2\ \ 2\ \ 2\ \ 2\ \ 2\ \ 1\ \ 2] \quad (11)$$

$$D = C\text{-}1 = [1\ \ 1\ \ 1\ \ 1\ \ 1\ \ 1\ \ 0\ \ 1] \quad (12)$$

D shows number of intercellular movement of each part

E = D′(transpose of). Transpose helps in matrix multiplications to achieve fitness function value.

$$F = N \times E = 80 \quad (13)$$

Fitness function value for above chromosome is 80 which is total number of movement of different eight parts and quantity to be manufactured, of each part per day is ten. An initial population of ten chromosomes is generated randomly which is called parent generation and fitness function value of each chromosome is calculated using same procedure as discussed from (1) to (13) in which (3) changes for each individual in each generation. (11) Shows the parent generation and fitness function value of each individual

P (0) is initial population or Parent generation

$$P(0) = \begin{array}{c} 1 \\ 2 \\ 3 \\ 4 \\ 5 \\ 6 \\ 7 \\ 8 \\ 9 \\ 10 \end{array} \begin{bmatrix} 1 & 3 & 2 & 3 & 2 & 1 & 3 & 2 \\ 3 & 1 & 2 & 3 & 2 & 1 & 1 & 2 \\ 2 & 1 & 3 & 2 & 3 & 1 & 1 & 2 \\ 3 & 2 & 1 & 3 & 2 & 2 & 1 & 3 \\ 2 & 3 & 1 & 1 & 2 & 3 & 2 & 1 \\ 2 & 2 & 3 & 1 & 2 & 3 & 1 & 1 \\ 3 & 2 & 3 & 2 & 1 & 3 & 2 & 1 \\ 2 & 3 & 2 & 3 & 1 & 2 & 1 & 3 \\ 3 & 2 & 3 & 1 & 3 & 2 & 2 & 1 \\ 1 & 2 & 3 & 2 & 1 & 3 & 3 & 2 \end{bmatrix} \begin{array}{c} 50 \\ 70 \\ 80 \\ 100 \\ 80 \\ 110 \\ 70 \\ 100 \\ 90 \\ 110 \end{array} \quad (14)$$

Fitness function value of each chromosome is calculated using same procedure with the help of MATLAB and objective function values are [50, 70, 80, 100, 80, 110, 70, 100, and 90,100] and average fitness function value of parent generation is 86. Fig. 3 shows the graph between chromosomes and fitness function values.

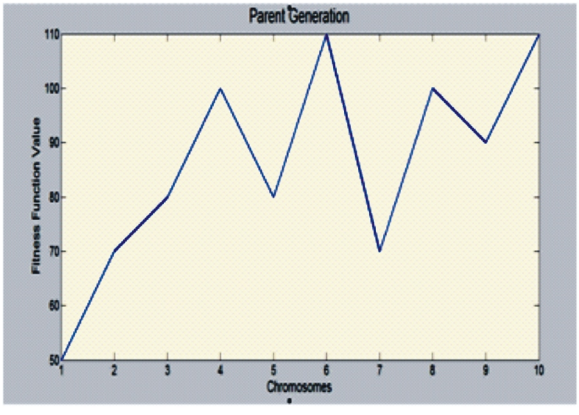

Fig. 3. Chromosomes Vs Fitness Function Values

3.2 Parent Generation

In parent generation two chromosomes with best fitness value are called elite chromosomes. In initial population chromosome 1 and 2 are elite children because they have minimum objective function values 50 and 70. Elite chromosomes remain unchanged in next generation and genetic operator operates (mutation and cross over) participate in reproduction of 1st generation. There are two approaches for mutation and cross over namely 'Rolette wheel selection' and 'random approach'. In this problem random approach is used because of small size of each individual and population. Mutation and crossover point is selected randomly in each generation. Cross over is exchange of genes in two chromosomes it can be explained by given example.

Before Crossover

Parent 01 2 1 3 2 3 | 1 1 2

Parent 02 3 2 1 3 2 | 2 1 3

After Crossover

Child 01 2 1 3 2 3 2 1 3

Child 02 3 2 1 3 2 1 1 2

Mutation always occurs in single chromosome and point of mutation is selected randomly. Mutation can be explained with example given below

Before Mutation

Parent 2 2 3 2 3 2 1 3

After Mutation

Child 2 1 3 2 3 2 1 3

In parameter settings it was clear that there are six chromosomes on which cross over is to be performed and there are only two chromosomes on which mutation occurs for production of next generation. Table II shows processes mutation and cross over on all individual of parent's generation.

TABLE II
1ST GENERATION CREATION PROCESS

P(0)	Cross over	Mutation	1st Generation
13232132	13232132	13232132	13232132
31232112	31232112	31232112	31232112
21323112	21323213	21323213	21323213
32132213	32132112	32132112	32132112
23112321	23112321	23212311	23212311
22312311	22312311	22313321	22313321
32321321	32321213	32321213	32321213
23231213	23231321	23231321	23231321
32313221	32313332	32313332	32313332
12321332	12321221	12321221	12321221

After mutation and crossover chromosomes modify their genes positions and generate children chromosomes. Same procedure is followed for generation 1 and objective function value is calculated.

3.3 Evaluation of Generation

Fitness function values of each individual in 1st generation are: [50, 70, 60, 110, 60, 100, 60, 50, 80, and 50] and average value of fitness function for generation 1 = 69. In 1st generation fitness function value is reduced as compared to parent generation and shown in Fig. 4.

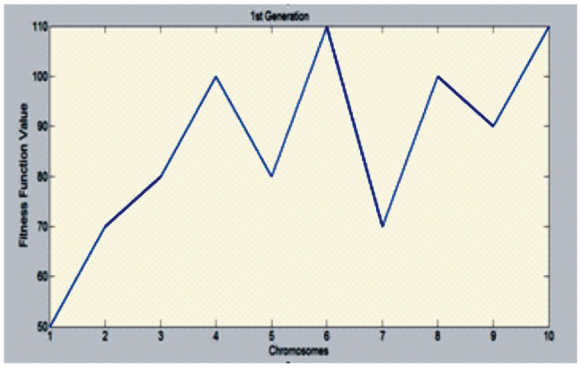

Fig. 4. Chromosome Vs Fitness Function Value

1st Generation

It is clear from Fig. 4 that fitness function values are less as compared to parent generation this due to evolution in generations as explained by Darwin's. According to Darwin theory of natural selection process everything passes through the emulation and changes its structure. Comparison of parent and 1st generation is explained in Fig. 5.

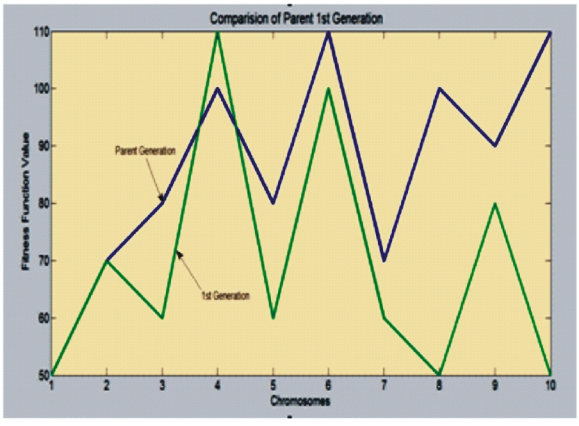

Fig. 5. Comparisons of Parent and 1st Generation

After mutation and cross over and selection of elite children next generation has been created and following the same procedure, total of 10 generations were generated, and fitness function value was reduced to minimum values at 10th generation because higher generations were repeating the same results as calculated previously.

IV. Results And Discussion

Evaluation process of all generation resulted into best fitness values at 10th generation and individual at same generation have minimum fitness function values. Minimization of fitness function values was due to genetic operators i.e. mutation and cross over. Weakest genes in chromosomes died as a result of evaluation. Parent and 10th generation with fitness function values are given below in Table III.

TABLE III
Comparison of Fitness Function Value

Parent Generation	Fitness Function Value	10th Generation	Fitness Function Value
13232132	50	32121321	50
31232112	70	12323222	50
21323112	80	31232132	40
32132213	100	13232112	50
23112321	80	21133113	50
22312311	110	32322212	70
32321321	70	21311311	80
23231213	100	23222321	50
32313221	90	22321213	60
12321332	110	32311231	80

Parent & 10th Generation

Comparison of parent and 10th generation can also be observed in Fig.6.

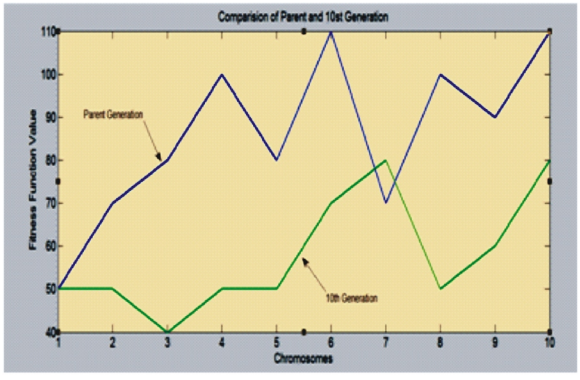

Fig. 6. Chromosomes Vs fitness Function value

In Fig. 6. it is clear that in 10th generation 3rd chromosome showed minimum value of fitness function value which is encoded to get cells as shown in Fig.7.

For chromosome: **3 1 2 3 2 1 3 2**

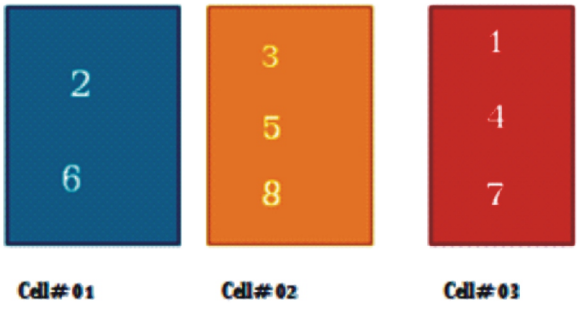

Fig. 7. Cell formations for minimization of intercellular movements

Fig. 11. Shows the cells and machines in cells. Now machine 2 and 6 are in cell 1, machine 3, 5 and 7 are in cell 2 and machine 1, 4 and 7 are in cell 3 respectively. This arrangement of machine cells shows the minimum movements of parts within different cells and total movements of parts in this type of arrangement is 40. The arrangement of machines in cells in Fig. 3 showed total that movement of parts in cell is 80 but solution proposed by GA reduced the cellular movements up to 50% which ultimately reduces cost of manufacturing, material handling cost and fatigue of workers.

V. Conclusion

The results from above discussion disclosed substantial advantages of genetic algorithm over traditional optimization technique. GA is quick and efficient algorithm to solve complex optimization problem. The reduction in intercellular movements of parts in shop increases the utilization of organization,

reduces the fatigue of workers, and reduces the material handling cost. Fifty percent (50%) reduction in intercellular movements is due to just changing the position of machines. Genetic algorithm is not just limited to one solution instead it gives multiple solution and it is easier for manager to pick the best solution that suits to organization keeping in view economic and technical issues. In installation of machinery in an organization some objectives can be set and depending upon this objective proper arrangement of machines can be carried out with the help of GA. Ability of GA to solve multiple objective problems makes it versatile. It is recommended that GA is advance tool for cell formation to achieve the desired objectives to increased productivity of organization.

REFERENCES

[1] Y. Zhang, "Cellular Manufacturing Systems," *Methods in Product Design: New Strategies in Reengineering,* p. 1027, 2013.

[2] N. Safaei, M. Saidi-Mehrabad, and M. Jabal-Ameli, "A hybrid simulated annealing for solving an extended model of dynamic cellular manufacturing system," *European Journal of Operational Research,* vol. 185, pp. 563-592, 2008.

[3] R. Tavakkoli-Moghaddam, N. Javadian, A. Khorrami, and Y. Gholipour-Kanani, "Design of a scatter search method for a novel multi-criteria group scheduling problem in a cellular manufacturing system," *Expert Systems with Applications,* vol. 37, pp. 2661-2669, 2010.

[4] A. A. Bulgak and T. Bektas, "Integrated cellular manufacturing systems design with production planning and dynamic system reconfiguration," *European Journal of Operational Research,* vol. 192, pp. 414-428, 2009.

[5] I. Mahdavi, A. Aalaei, M. M. Paydar, and M. Solimanpur, "Designing a mathematical model for dynamic cellular manufacturing systems considering production planning and worker assignment," *Computers & Mathematics with Applications,* vol. 60, pp. 1014-1025, 2010

[6] V. Deljoo, S. Mirzapour Al-e-hashem, F. Deljoo, and M. Aryanezhad, "Using genetic algorithm to solve dynamic cell formation problem," *Applied Mathematical Modelling,* vol. 34, pp. 1078-1092, 2010.

[7] M. A. Bajestani, M. Rabbani, A. Rahimi-Vahed, and G. Baharian Khoshkhou, "A multi-objective scatter search for a dynamic cell formation problem," *Computers & operations research,* vol. 36, pp. 777-794, 2009.

[8] A. Tariq, I. Hussain, and A. Ghafoor, "A hybrid genetic algorithm for machine-part grouping," *Computers & Industrial Engineering,* vol. 56, pp. 347-356, 2009.

[9] S. Sofianopoulou, "Formation of manufacturing cells in group technology using a genetic algorithm approach," *International Journal of Industrial and Systems Engineering,* vol. 5, pp. 212-225, 2010.

[10] A. Sadrzadeh, "A genetic algorithm with the heuristic procedure to solve the multi-line layout problem," *Computers & Industrial Engineering,* vol. 62, pp. 1055-1064, 2012.

[11] G. Aiello, G. La Scalia, and M. Enea, "A multi objective genetic algorithm for the facility layout problem based upon slicing structure encoding," *Expert Systems with Applications,* vol. 39, pp. 10352-10358, 2012.

[12] M. Jahanzaib, S. Nadeem, et al.(2013)." Application of Genetic Algorithm (GA) Approach in the Formation of Manufacturing Cells for Group Technology. *Life Science Journal*, 9 (4), 799-809

Comparison of Water Conveyance Losses in Unlined and Lined Watercourses in Developing Countries

T. Sultan[1], A. Latif[2], A. S. Shakir[3], K. Kheder[4], M. U. Rashid[5]

[1,2]*Department of Civil Engineering, University College of Engg. & Tech. BZU. Multan, Pakistan*
[3]*Department of Civil Engineering, University of Engineering and Technology, Lahore. Pakistan*
[4]*Department of Civil Engineering Department, College of Engineering, Salman bin Abdulaziz University, P. O. Box 655, AlKharj 11942 Saudi Arabia*
[5]*Senior Engineer, NESPAK, Lahore, Pakistan*
[1]tahirsultanch@hotmail.com

Abstract-Open conduits are the main systems for supplying irrigation water in developing countries. However, most of these schemes are frequently criticized for their low conveyance efficiencies. Under the water scarce situation, improving the conveyance efficiency offers an opportunity to realize basin level water savings. To define the significance of such opportunities, it is essential to identify the reason, location and conveyance losses in the tertiary canals that can be saved.The operationalcost of running canals have also been significantly reduced through savings in the conveyance infrastructures. The other benefits that may be attained are equitable water distribution and avoiding tail shortages.Lining of main watercourses attempts to save good quality canal water, which is used by all the share holders of the command.This paper mainly explains conveyance losses evaluation in the unlined and lined tertiary channels irrigation supply system situated in South Asia (Pakistan and India). The results indicate that in Pakistan almost 43.5% of the water losses occur in lined watercourses and 66% losses in unlined watercourses and in India 11% of water losses occur in lined watercourses and 20-25% in unlined watercourses. The conveyance losses in Turkey and Egypt have also been elaborated in the study for the purpose of comparison. The results indicate that the conveyance losses in tertiary irrigation system in Pakistan are high. Moreover, good quality lining and proper operation/maintenance are necessary for better effectiveness and sustainable water management.

Keywords-Cellular Manufacturing, Cross Over, Elitism, Genetic Algorithm, Mutation, Population, cell formation

I. INTRODUCTION

Open channels system is the main water supply intervention in the irrigation scheme in most regions around the world and it will remain as the central technique in the predictable future as well. However, a majority of these conveyance schemes are often criticized for their water conveyance losses. In irrigation network serviced by watercourses, conveyance losses are defined, the difference between water delivered to the irrigation system and water delivered to the nakkas. These conveyance losses fluctuate from year to year because of variations in operational methods, water accessibility, customer demands and climate.

Irrigation is one of the essential inputs required for sustainable irrigated agriculture in many countries. Watercourse distribution in developing countries is not equitable. Under the existing situation, the farmers of head reaches of irrigation channels (watercourses) receive more water than the tail reaches farmers. The conveyance losses had a remarkable effect on water distribution; as conveyance losses at the head sections were reduced, farmers were getting more discharge at their farm gates [1]. Thus there is a need to quantify this difference in terms of income to the farmers. Canal irrigation systems in numerous parts of the world are known to be performing well below their potential (ICID past president).

Major conveyance losses in watercourses are due to seepage. Efficient water saving can be achieved by keeping the conveyance losses to a minimum level. Large amount of water is lost during its route up to the farms level, especially the conveyance losses are pronounced at tertiary (watercourses) level of the irrigation system in Pakistan and India. The main reasons for conveyance losses in watercourses are leakages from turnouts, high density of vegetation in the unlined watercourses, turns in the watercourse, un-compacted and weak banks, deposition of sediments, siltation, holes made by rodents and lack of maintenance [2]. Reference [3] narrated that 40% of the total water supply is lost in the canals and watercourses before reaching the farm gate. Reference [4] reported that less irrigation supplies than its desired share is the main cause of the low productivity; out of

many reasons seepage and percolation from the canals and watercourses are the major one.

Lining of tertiary canals has been commonly practiced in the world for enhancing conveyance efficiency and saving water. Lining of tertiary canals is one of the main on-farm water management interventions. The lining results in curtailing the seepage from the tertiary canals. The seepage can be decreased to less than 25 percent of the total losses. Decreasing seepage losses results in saving of water and accordingly more water is available for irrigation at farm gate that can increase the cropped area and the crop yield. Lining is a long term effective technique for reducing seeping losses from the watercourse, but on account high cost; it is somehow provided only on 15-30% length at the head of several watercourses in Punjab province of Pakistan [5]. Lining has increased 25% conveyance efficiency and if we lined all other watercourses, it will not only enhance conveyance efficiency but will also help in equal water distribution among farmers and increase the command area of that watercourse [6]. Reference [7] compared the water conveyance losses between lined and unlined tertiary canals of Indus Basin of Pakistan. Four watercourses were selected for the study with two lined and two unlined watercourses. Conveyance losses were evaluated by inflow-outflow method using cut-throat flumes. The study concluded that lining decreases water conveyance losses by 22.5%. IWASRI [8] reported the studies carried out by Watercourse Monitoring and Evaluation Directorate of WAPDA. According to that water losses measurements were made on 26 watercourses of which 10 were lined (brick lining) and 16 were unlined. On the lined watercourses a net increase of 12-14% in the conveyance efficiency was found from head to tail reach.

The another intervention of enhancing irrigation supplies through decreasing water “losses” from watercourses by choosing lining has been gradually adopted in India. Subsequently, tertiary canal conveyance losses in a complex distribution system in alluvial type soils are approximately one and a half times that of a main canal and three times that of a distributary canal. The lining of tertiary canals has been comprised by the engineering civic as a means of confirming water deliveries to the “unreached” in the tail end regions [9]. Methods have been developed for augmenting the length of a tertiary canal to be lined to curtail cost [10]. Channel lining is suggested in salty groundwater regions. Tertiary canal lining was known as an actual intervention to decrease seepage losses since more water losses occurred at this level of the water conveyance system [9]. Reference [11] stated that in the absence of proper lining, about 1035% of water is lost during conveyance from the source to the field due to seepage and evaporation losses.

The measured discharge values from watercourses of distributaries in Sirsa district in India revealed a significant seepage loss of about 33% for lined and 48% for unlined watercourses [12]. Reference [13] reported that at tertiary level, seepage losses are evaluated 11% and 2025% in the lined and unlined watercourse, respectively.

The objective of the present paper is to study the conveyance losses in lined and unlined watercourses of Pakistan and India. This paper also explores conveyance losses and the saving of water by lining and thus, enhancing conveyance efficiency.

II. Areas of Study

The tertiary canal irrigation system in the world is facing a number of operational problems resulting in more losses of water during conveyance and of irrigation water to agricultural lands. These water losses result in constrained water deliveries of canal water. Water losses from these canals have major impacts on surface water supplies and needs management, and must be minimized, if not altogether eliminated. This is perhaps the most cost-effective method of augmenting water supplies (IDWR 2005).

The problem of conveyance losses through irrigation systems has a major impact on on-farm water management and surface water supplies. While a number of international and national organizations have endeavored to evaluate the losses from the tertiary canals, the effect of lining on the water losses have not been addressed widely. The main areas focus in the study for estimating conveyance losses in lined and unlined watercourses are Pakistan and India.

Pakistan

In Pakistan, the water losses in unlined and lined tertiary canals of Indus Basin have been reviewed. Indus Basin Irrigation System (IBIS) of Pakistanis the strong heart of the country's economy. Pakistan is mostlysemi-arid and arid with less water resources. The agriculture zone in Pakistan is the major consumer of water. Approximately 97 percent of all river water is being used for farming. Several researchers concluded that reducing loss of water from watercourses carrying water from distributary/minor to farmers' fields is one of Pakistan's highest potentials for enhancing supplies delivered to those fields. The irrigation system comprises of a network of main canals, branch canals, distributaries and watercourses. Conveyance losses in the distributaries and watercourses are abouttwenty five and thirty percent respectively. Because of lack of adequate drainage infrastructure and constant percolation and seepage from distributaries and field channels, water-logging and soil salinity inflict severe threats to the irrigated regions.

Lining is a current activity in many irrigated regions of Pakistan that is focused by a number of factors including: contingent liability for water-logging of land adjacent to channels or flooding, accessions to salt mobilization and shallow water tables and water savings. Lining of watercourses is also

expected to increase productivity by efficient utilization of resources, improved irrigation facilities, strengthened farmer's participation in the management of water, and generally promoted condition for progress of the rural areas.

The comparison of water losses between lined and unlined tertiary canals of Indus Basin in Pakistan indicates that for the tested unlined watercourses, water losses ranged from 64 to 68%.

India

Irrigation system has acquired augmenting significance in agriculture internationally. From impartial 8 million hectares (M Ha) in 1800, irrigated area across the world augmented fivefold to 40 Million Hectares (M Ha) (13.4 M Ha in India) in 1900, to 100 M Ha in 1950 and to just over 255 M Ha in 1995. With approximately one fifth of that area (50.1 M Ha net irrigated area), India has the highest irrigated land all over world nowadays (Postel, 1999).

In India the conveyance losses in lined and unlined tertiary canals of Haryana have been reviewed. Haryana is a frequently water-scarcity state in India. 80% of the farmingregion of the state (2.8 million hectares) is irrigated. The extent of area irrigated by canal water is approximately the same as that area irrigated by groundwater and in many instances, conjunctive intervention is adept.

The two main canal systems of the state are the Western Yamuna canal system, which is served from the Yamuna River and the Bhakra canal system, which takes its supply from the Indus basin.

Old earthen irrigation tertiary canals in permeable soils can lose a lot of water through seepage in India. Large losses through the bed and sides of canal lead to low conveyance efficiency; that is, (the ratio of water reaching farm turnouts to that released at the source of supply from a river or reservoir). Earthen canals also get clogged up with weeds which reduce the water-carrying capacity.

In unlined channels, only a portion of the water supplied at the canal head reaches the farmer's field. The main loss is through seepage. The commonly accepted figures for conveyance losses in alluvial plains of north India (Ganga basin) are 17% for main and branch canals, 8% for distributaries and 20% for water courses (Report of the Irrigation Commission, 1972).

In addition to Pakistan and India, the conveyance losses of lined and unlined channels in tertiary irrigation system of Egypt and Turkey have been reviewed. The conveyance losses in lined and unlined channels in tertiary irrigation system are 13 and 20 % in Egypt while 10 and 27 % in Turkey (Dennis Wichelns, 1999; Mohamed et al., 1995;ErhanAkkuzu et al., 2006).

III. Results and Discussions

Results

Table 1. provides the comparison of conveyance losses in developing countries:

Discussions

Comparing the average water loss from lined and unlined tertiary canals, it can be assessed that the lining reduces water conveyance loss significantly in developing countries. In developing countries like Pakistan and India, lining of watercourses increases the conveyance efficiency by 22.5% and 12% respectively. Similarly in Turkey and Egypt, lining impact is that it reduces the conveyance losses by 17 and 7% respectively. It may be concluded from the Table 1 that only lining intervention of tertiary irrigation channels result in substantial reduction of conveyance losses and accordingly enhancing the conveyance efficiency. Also the improvement of conveyance efficiency of water courses significantly contributes in overall irrigation system upto farm level.

TABLE 1
Comparison of Conveyance Losses in Developing Countries

Country Name	Irrigated Land (km2)	Conveyance Losses (%)		Conveyance Efficiency (%)		%age enhance in conveyance Efficiency due to lining	Source
		Lined Water Courses	Unlined Water courses	Lined	Unlined		
Pakistan	198,700	43.5	66	56.5	34	22.5	Arshad et al.(2011)
India	622,860	11	23	89	77	12	Ambast et al. (1990)
Turkey	52,150	10	27	90	73	17	ErhanAkkuzu et al. (2006)
Egypt	35,300	13	20	87	80	7	Dennis Wichelns. (1999); Mohamed et al. (1995)

However, it can be improved by adopting lining option coupling with other interventions at farm level i.e. bed & furrows and zero tillage etc.Moreover, the lining of distributaries and minors (secondary irrigation system) must be evaluated and done to further enhance the conveyance efficiency of irrigation system. Recently, Provincial irrigation and Agriculture departments in Pakistan have recognized the fact of huge benefits of lining of irrigation system (secondary and tertiary) and initiated several projects for lining, improvement, rehabilitation and remodeling of secondary and tertiary irrigation system upto farm level i.e. Mega Irrigation Projects Punjab, Punjab Irrigation system Improvement Project, Irrigation Systems Rehabilitation Project, Rehabilitating Lower Chenab Canal System Project , Lining of Distributaries and Minors in Punjab, Lining of Distributaries and Minors in Sindh, Twenty Small Irrigation Schemes in Balochistan, Remaining Punjab Irrigated Agriculture Investment Programme and Water Conservation and Productivity Enhancement Through High Efficiency Irrigation Systems. The regular and proper operation and maintenance of irrigation system is necessary to achieve the desired objectives. Most of these projects were started after 2005 and now at different stages of execution, even some of the projects are near completion. These projects are scattered all over Pakistan in all the four provinces. After the successful completion of these projects, the conveyance efficiency of overall irrigation system will substantially enhanced. It will also improve the crop yield, crop intensity, water productivity, gross and net benefits.

The proper operation of irrigation system also involves running the channels at design discharge to maintain the desired full supply level, velocity and other hydraulic parameters. The proper hydraulic parameters tend to keep the channel in "neither silting nor scouring" state. It results in equitable water distribution and avoiding tail shortages. Improving conveyance efficiency also results in reducing water theft as the farmers of head, middle and tail reaches get their desired share of water.

The reasons identified for excess loss of water through the tertiary canalsare due to eroded mortar, cracks and structural failure of the lined banks. The capacity of tertiary canal also decreases due to silting, resulting in overtopping of flows at many sites.

V. Conclusions

The canal irrigation scheme, especially, the tertiary system is facing a number of operational problems resulting in high losses of water during its conveyance.

The extra leakage of water through the tertiary canals is probably due to eroded mortar, cracks and structural failure of the lined banks. In addition, the capacity of tertiary canal is also curtailed due to silting, resulting in overtopping of flows at many sites.

The reason of the less conveyance efficiency in unlined portion of the watercourses was absolutely due to lack of proper maintenance of the watercourses hence more seepage and leakage losses presence of vegetation, improper alignment of the watercourses and rodent effect.

In developing countries i.e. Pakistan and India, lining of watercourses increases the conveyance efficiency by 22.5% and 12% respectively. The lining of watercourse effectively save the water losses and ultimately needs proper maintenances and cleaning otherwise losses will be higher than the normal.

VI. Recommendations

As a result of this study and from the perusal of other pertinent literature review work, the following recommendations are suggested for minimizing the losses in conveyance system and for improvement of watercourses.

The liningof channelshouldbe decided on the extent of seepage losses.

Frequent maintenance and cleaning of earthen watercourses are necessary to maintain high conveyance efficiencies. Proper improvement with bricks, concrete lining, with naccas and check may be done so as to save high amount of water lost through seepage, rodent holes and other losses etc.

Selection of lining for tertiary channels may be based on factors in addition to cost/benefit ratios and delivery efficiencies, such as the ability of the lining to manage and observe water and soil.

Therefore, it is recommended that watercourses must be lined for better effectiveness and sustainable water management.

References

[1] T. Sarwar, M. Jehangir and M.J. Khan. 2001. Effect of watercourse maintenance and variable discharges on conveyance losses and water distribution. *Sarhad J. Agric. 17:387-394.*

[2] J. Zeb, S. Ahmad, M. Aslam and Badruddin. 2000. Evaluation of conveyance losses in three unlined watercourses of the Warsak Gravity Canal. Pak. J. Biological Sciences 3(2): 352-353.

[3] A. Maqbool, and Abdullah, 2006. Environmental hazards. "Daily Dawn" the Internet Edition, January 30, 2006.

[4] F. Munir, 2003. Constraint Analysis to improve Irrigation efficiency at farm level. A Case Study of District Sahiwal. M. Sc. (Hons.) Thesis, Dept. of Rural Soc., Univ. ofAgri., Faisalabad.

[5] OFWM. 2005. A study on alternatives of watercourse lining. Directorate General Agriculture (Water Management), Punjab, Lahore.

[6] M. Arshad and N. Ahmad. 2011. Performance assessment of irrigation system in rice-wheat cropping zone using modern techniques. *ICID 21st International Congress on Irrigation and Drainage, 15-23 October 2011, Tehran, Iran.*

[7] M. Arshad, N. Ahmad, M. Usman and A. Shabbir. 2009. Comparison of water losses between unlined and lined watercourse in Indus Basin of Pakistan. Pak. J. Agri. Sci. 46:280-284.

[8] IWASRI. 2004. Impact of Watercourses Lining on Reducing Drainage Requirement. International Water logging and Salinity Research Institute. Publication 258. WAPDA, Lahore. Pakistan.

[9] National Seminar. 1983. *Focus on lining of watercourses in canal command areas*. Chandigarh, India: Haryana State Minor Irrigation (Tube Wells) Corporation.

[10] S. P. Malhotra, 1975. Optimum length required to be lined in a watercourse. *The Annual Journal, The Institution of Engineers (India), 5257. Chandigarh, India: Punjab, Haryana & Himachal Pradesh Center*.

[11] R. P. Singh, and M.A. Khan, (1999) Rainwater management: water harvesting and its efficient utilization. In: H.P. Singh, Y.S. Ramakrishna and B. Venkateswaralu.

[12] Tyagi, (1996) Improving canal water delivery performance: some approaches, Research Bulletin No 246, Central Board of Irrigation and Power, New Delhi, p 69.

[13] S.K. Ambast, N.K. Tyagi and H.R. Tyagi, 1990. Performance evaluation of water delivery system in a unit command area. *J. Ind. Water Resour. Soc. 10 (2), 1924.*

[14] IDWR. 2005. Augmenting Water Resources. Water in Rajasthan. Report of the Expert Committee on Integrated Development of Water Resources, India.

[15] S. Postel, 1999. Pillar of Sand: Can the Irrigation Miracle Last? New York & London: WW Norton & Company.

[16] *Report of the Irrigation Commission*, Volume-I, 1972.

[17] W. Dennis, 1999. A cost recovery model for tertiary canal improvement projects, with an example from Egypt. Agricultural Water Management 43 (2000).

[18] F. B. Mohamed and A.A. Awan. 1995. Practical Estimation of Seepage Losses along Earthen Canals in Egypt. *Research Institute of Channel Maintenance, National Water Research Center, El-Kanater El-Khaireia, Kalubeia, Egypt.*

[19] A. Erhan, H. B. Unal, B. S. Karatafi, 2006. Determination of Water Conveyance Loss in the Menemen Open Canal Irrigation Network. *Turk J Agric For 31 (2007) 11-22.*

Effect of Concrete Strength on Behavior of Strip Confined Columns

M. F. Tahir[1], Q. U. Z. Khan[2], A. Ahmad[3]

[1,2,3]Department of Civil Engineering, University of Engineering & Technology, Taxila
[1]fiaz.tahir@uettaxila.edu.pk
[2]dr.qaiser@uettaxila.edu.pk

Abstract-This study presents the cyclic axial test results of ten 150×150×600mm RCC columns confined with standard stirrups and mild steel strips of size 2×15mm (Strip-14), 1.6×19.77mm (Strip-16) and 1.28×18.8mm (Strip-18) . Columns were divided in two groups. In group "A" columns concrete strength was 27MPa and in group B columns it was 34 MPa. Strength of concrete used in group "B" column was 26% higher than group "A" columns. Test results revealed that by 26% increasing concrete strength, resulting increase in axial capacity of group B columns confined with stirrups, strip-14, 16 and 18 was respectively 22, 27, 21 and 43 %.

Keywords-columns, confinement, axial strength, stirrups, strips

I. INTRODUCTION

Factors that can improve confinement include [1]-[6], the following:-

1- Spacing of confining steel
2- Additional overlapping hoops and ties.
3- Even distribution of main column bars around perimeter.
4- Increasing the ratio of volumes of transverse reinforcement to volume of concrete core.
5- Improving grade of confining steel
6- Providing spirals, circular ties or strips instead of rectangular ties and cross hoops

Confinement can also be improved by increasing the diameter of wires and decreasing spacing of spirals [6]. Additional parameters that can improve performance of confining steel include proper detailing of confining reinforcement, concrete compressive strength and type of aggregate [6]. Researchers [1], [2], [7] discovered that strength and ductility can be improved by distributing the longitudinal steel around the core. They also found that by supporting each longitudinal bar with cross ties and hoops confinement can be increased. References [8] and [9] reached at the same conclusion. Welded wire fabric can also increases the strength by 40 [10], however improvement in ductility can be achieved only if it is used with ties at d/2 spacing. Reference [8] investigated in detail the affect of following parameters:-

1. Arrangement of main bars in columns
2. Quantity of confining steel and main bars
3. Arrangement of ties.
4. Spacing of ties
5. Properties of lateral steel

It was also discovered that ties if properly placed in column also worked well up till their final fracture. Reference [11] studied the behavior of columns confined with prestressed metal strips in terms of stress strain relation. It was found that active confinement in addition to improvement in strength and ductility can result in stiffer pre-peak response of concrete specimen. Stress-strain curves of specimen are important because these give an overview that whether confinement has increased the ductility and strength [6]. Researchers have found that diameter and yield strengths of confining steel, volumetric ratio of confining reinforcement to concrete core and arrangement of confining steel as well as longitudinal steel significantly affect stress strain relation of columns.

It was also found that both strength and ductility can be improved by replacing stirrups with strips [12]. However when width thickness ratio of strips increases by 12% the improvement in strength is less as compared to ductility. Refrence [6] found that performance stirrup confinement can be improved by concrete compressive strength. This paper investigates the effect of concrete strength on the behavior of strip confined RCC columns.

II. TEST PROGRAM

Columns were tested in two groups, A and B containing five columns in each group. In each group one column was provided with four 6.35mm diameter longitudinal bars and it was confined with 6.35mm diameter standard stirrups. Remaining three columns were confined with mild steel strips of three different width thickness ratios of 7.5, 12.4 and 18.8. It is

important to mention here that width and thickness of each strip was selected to achieve cross-sectional area equivalent to 6.35mm diameter deformed bars. Fifth column was cast without any reinforcement. Identification numbers and cross sectional properties of strips are presented in Table I.

TABLE I
CROSS-SECTIONAL PROPERTIES AND IDENTIFICATION NUMBER OF STRIPS

S. No.	Identification number	Thickness (mm)	Width (mm)	Width thickness ratio of strips
1	14	2.00	15	7.5
2	16	1.6	19.77	12.4
3	18	1.28	25	18.8

In group-B columns concrete strength was 34MPa instead of 27MPa rest all parameters were same. Identification name of each column of these two groups and corresponding types of confinement used are shown in group.

Table II. In column 3 of table first letter represents that type of confining steel used and second letter corresponds to the name of group.

TABLE II
SPECIFICATION OF SPECIMEN COLUMNS

Column No. (1)	Group (2)	Identificat-ion name of column (3)	Concrete Strength (Mpa) (4)	Type of confinement (mm) (5)
1	Group A	P-A	27	-
2		S-A	27	6.35mm ties
3		14-A	27	15mm strips
4		16-A	27	19.77mm strips
5		18-A	27	25mm strips
6	Group B	P-B	34	-
7		S-B	34	6.35mm ties
8		14-B	34	15mm strips
9		16-B	34	19.77mm strips
10		18-B	34	25mm strips

III. MATERIAL PROPERTIES

In this experimental program three types of materials were used, 6.35mm diameter deformed rebars, strips of different thicknesses and concrete. Tension test on strip material was performed on the coupons cut from plates as per Standard Test Methods for Tension Testing of Metallic Materials "E 8M-04" using MTS 810, Universal High Frequency Fatigue Testing Machine (UHFFT Machine). Fig. 1. presents the stress strain relationship of each test specimen. Yield and ultimate strength of testes coupons is shown in Table III.

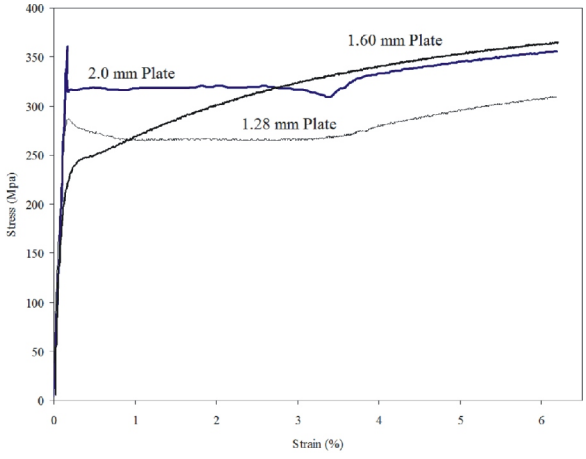

Fig. 1. Stress strain relationship strip material

TABLE III
PHYSICAL PROPERTIES STRIP MATERIAL

S. No.	Strip Identification number	Yield strength (Mpa)	Ultimate strength (Mpa)
1	14	355	361
2	16	242	365
3	18	286	309

IV. STRUCTURAL DETAILING OF SPECIMEN

Structural detailing of columns is shown in Fig. 2-5. In strip and stirrup confined columns clear spacing of stirrup/strip ties were kept equal to 31mm. Clear cover to main bars was 13mm. this resulted in "d" for each column equal to 137 mm. In order to prevent damage of column due to accumulation of stresses near upper and lower machine jaws and avoid misleading results a 2×38mm mild steel collar was externally applied at the top as well as at the bottom of each column.

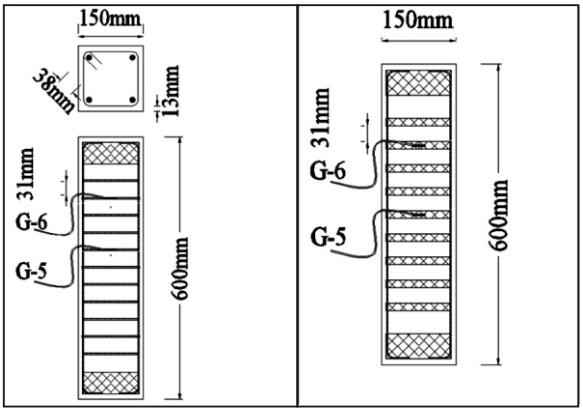

Fig. 2. Standard stirrup confinement

Fig. 3. 15mm strip confinement

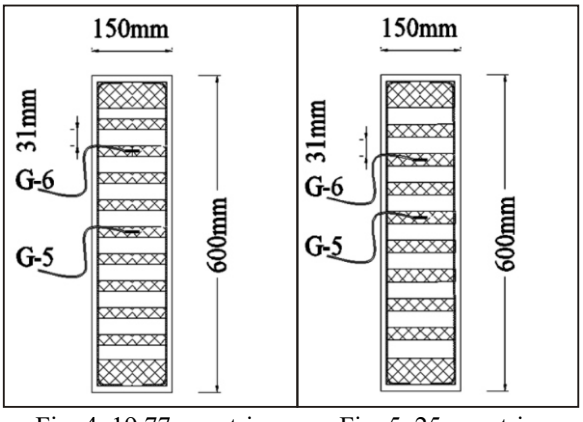

Fig. 4. 19.77mm strip confinement

Fig. 5. 25mm strip confinement

V. Instrumentations

Axial deformation in column was measured by two gauges gauge-1 and gauge-2 as shown in Fig. 6. Value of axial force at desired time intervals was measured by 200 ton load cell which was connected to data acquisition system.

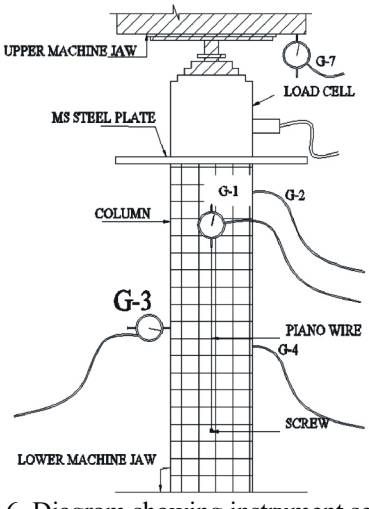

Fig. 6. Diagram showing instrument set up

Gauges 3. and 4. were installed to monitor any abnormal column response during testing. These were installed at mid points perpendicular to the left and rear face respectively. These gauges were also helpful in monitoring the cover spall off. Gauges and load cell were connected to a data logger in which displacement and load data was recorded automatically.

VI. Testing Methodology

Specimen were tested in UTM and cyclic axial load was applied during testing .Detail of load cycles applied is shown in Fig. 7. A view of the test lab during experimentation is shown in Fig. 8. All tests were displacement control type and loading rate and strains were controlled manually. During testing axial force was applied at 0.14 to 0.34 MPa/sec, as recommended by ASTM standard.

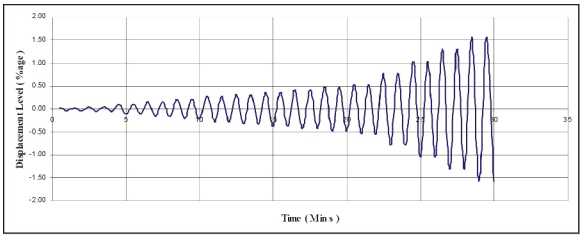

Fig. 7. Graphical representation of load cycles

Fig. 8. Test in progress in laboratory

VII. Analysis of Results

Stress strain behavior of both groups of columns was drawn up to 0.3% strain and is shown in Fig. 9. Stress strain curves of group A column are drawn in full line and that of group B column is shown in dashed lines.

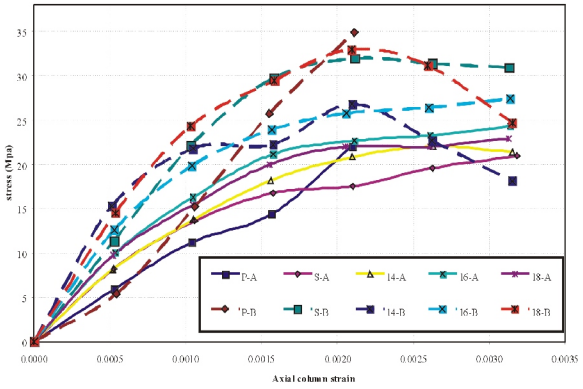

Fig. 9. Stress strain relation

It was observed that irrespective of concrete strength axial capacity of columns increased by increasing the strip widths. However it was reverse for columns confined with wider strips of lesser stiffness. As already mentioned in present study three different types of strip confinement were employed. Increase in widths to thickness ratio of strips has an affect on the stiffness of strips which reduces by decreasing the thickness and increasing the strip width. The resulting decreased stiffness is responsible for reduced confining effects as capacity of strips to resist lateral pressure exerted by lateral expansion of plain concrete reduces. This results in reduction of axial capacity of column with greater width to thickness ratios. It is obvious in figure 10 that axial capacity of column 18-A is 5% less than column 16-A.

Table IV compares the calculated and tested strength of columns in group A and B. In this table calculated axial capacity of column (P_{cal}) is calculated by using following relation:

$$P_{calc} = \alpha f_c^{'}\left(A_g - A_s\right) + A_s f_y \qquad (1)$$

TABLE IV
COMPARISON OF TESTED AND CALCULATED STRENGTHS

Column No.	Type	P_{test} (KN)	(P_{calc}) (KN)	P_{test}/P_{cal}
1	-	-	-	-
2	S-A	607.5	596.7	1.02
3	14-A	495.0	596.7	0.83
4	16-A	540.0	596.7	0.90
5	18-A	517.5	596.7	0.87
6	-	-	-	-
7	S-B	742.5	658.7	1.13
8	14-B	630	658.7	0.96
9	16-B	652.5	658.7	0.99
10	18-B	742.5	658.7	1.13

In above equation α is the ratio of unconfined concrete strength of plain concrete columns to the cylindrical strength. Value of α varies between 0.85 and 0.90 for large size samples [13-14]. In the present study, value of α was "0.93" and "0.82" for group A and B columns respectively.

A_g=Gross area of column

A_s=Area of longitudinal steel

f_y=Yield strength of steel

f_c=Strength of concrete cylinder at the time of testing

Just like group A, columns in group B also showed an increasing trend of axial strength with the increase of strip width. However P_{test}/P_{cal} ratio in columns confined with strip 18 and stirrups was same. Same trend was observed in columns of group A. It was found that axial capacity of columns increased by increasing concrete strength. In the present study the difference in concrete strength of group A and B column is 26% and resulting increase in axial strength of columns is 22, 27, 21 and 43% respectively for columns confined with stirrups, strip-14, 16 and 18 respectively. In addition to above the observed Increase in axial strength for columns confined with strip 18 is maximum, showing 20% strength increase as compare to an average increase in axial strengths of column confined with stirrups, strip-14, 16 and 18. It can be concluded from this research that by increasing column concrete strength increase in axial strength of columns is higher when wider strips are used.

VIII. CONCLUSIONS AND RECOMMENDATIONS

In this research it is found that strips improve both strength and ductility. Area of concrete core of column specimen was kept constant throughout this investigation however it is important to mention here that being less in thickness strip confinement covers more area of concrete core as compared to conventional stirrups. From experiments performed in present study following can be concluded:-

1. In the present study strength of concrete used in group "A" column was 26% higher than group B columns. Resulting increase in axial capacity of columns confined with stirrups, strip-14, 16 and 18 was 22, 27, 21 and 43 % respectively.
2. By 26 % increasing concrete compressive strength, axial strength of columns confined with strip-18 improved by 43 % as compared to an average increase of 23% when stirrups, strip14 and 16 are used.

REFERENCES

[1] J. Vellenas, V. V. Bertero, and E. P. Popov,"Concrete confined by rectangular hoops subjected to axial loads," Report 77/13, Earthquake Engineering Research Center, Univ. of California, Berkeley, Calif,1977.

[2] S. A. Sheikh, , and S. U. Uzumeri, "Strength and ductility of tied concrete columns," J. Struct. Div., A.S.C.E., 106(5), 1079-1102. 1980.

[3] B. D. Scott , R. Park , and M. J. N.Priestley, "Stress-Strain Behavior of Concrete Confined by Overlapping Hoops at Low and High Strain Rates," ACI JOURNAL, proceedings Vol. 79, No. 1, pp. 13-27, 1982.

[4] J. B. Mander, M. J. N. Priestley, and R. Park, "Seismic design of bridge piers," Research Report No. 84-2, Univ. of Canterbury, New Zealand, 1984.

[5] M. Rizwan, "Performance evaluation of RC structures under earthquake loading," Thesis (PhD) Civil Engineering Department UET Lahore, 2010.

[6] S. M. Ahmad, , and S. P. Shah, "Stress-strain curves of concrete confined by spiral reinforcement," Am. Concr. Znst. J., Vol. 79, No. 6, pp. 484-490, 1982.

[7] S. S. Sheikh, and S.M Uzumeri, "Strength and ductility of confined columns," Journal of the Structure Divisions ASCE, Vol. 106, No STS, pp. 1079-1102, 1980.

[8] R. Park , M. J. N. Priestley , and W. D. Gill, "Ductility of square-confined concrete columns," J. Struct. Div.,ASCE, Vol. 108, No.4, pp. 929-950, 1982.

[9] G. Ozcebe, and G. Murat, "Confinement of Concrete Columns for Seismic Loading," ACI Structural Journal, Vol. 84, No.4, pp. 308-315, 1987.

[10] S. R. Razvi, and M. Saatcioglu, "Behavior of Reinforced Concrete Columns Confined with Welded Wire Fabric and/or Rectilinear Ties," Research Report No. 8902, Department of Civil Engineering, University of Ottawa, pp. 103, 1989.

[11] H. Moghaddam , M. Samadi, P. Kypros and S. Mohebbi, "Axial compressive behavior of concrete actively confined by metal strips; part A: experimental study," Materials and Structures, 43,1369-1381, 2010.

[12] M. Fiaz T, "Performance of steel strip confined columns," thesis (PhD) Civil engineering Department UET Taxila, 2013.

[13] R. Park , and T. Paulay, "Reinforced concrete structures", John Wiley and Sons, New York, N.Y,1975.

[14] R. R. Saleem , M. Saatcioglu, "Confinement of reinforced columns with welded wire fabric," ACI Structural Journals, Vol. 86, No. 5,1989.

APPENDIX-A

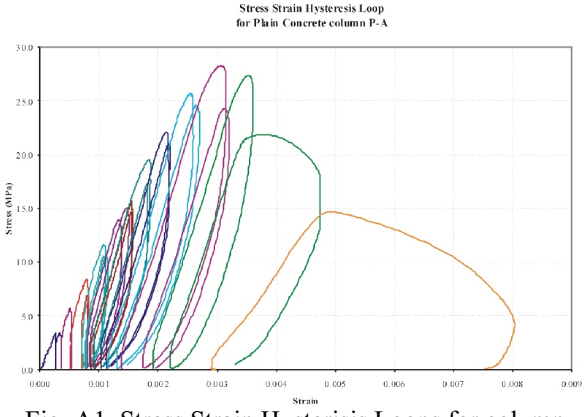

Fig. A1. Stress Strain Hysterisis Loops for column P-A

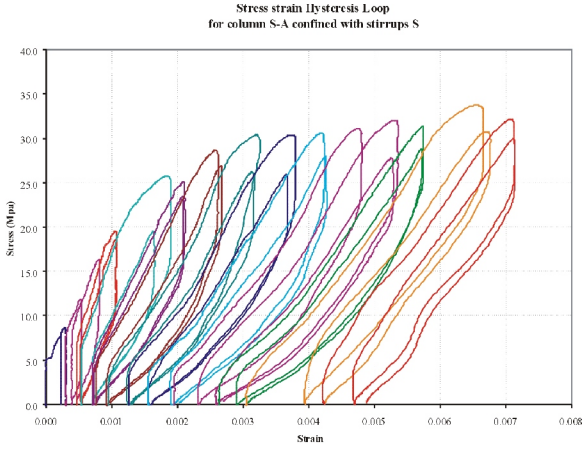

Fig. A2. Stress Strain Hysterisis Loops for column S-A

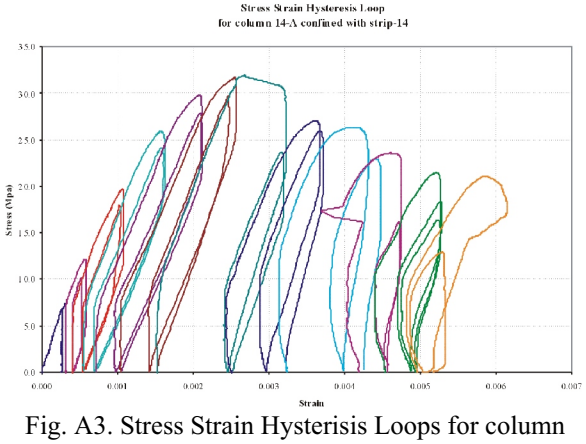

Fig. A3. Stress Strain Hysterisis Loops for column 14A

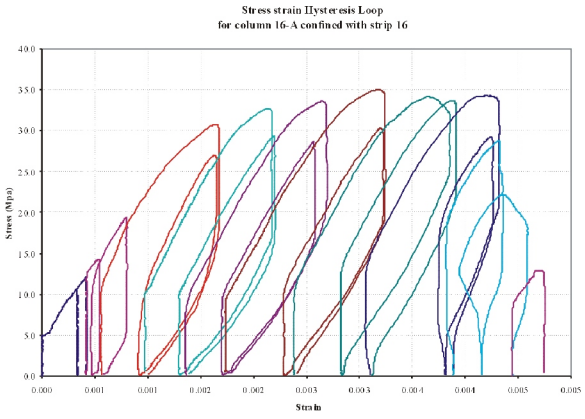

Fig. A4. Stress Strain Hysterisis Loops for column 16-A

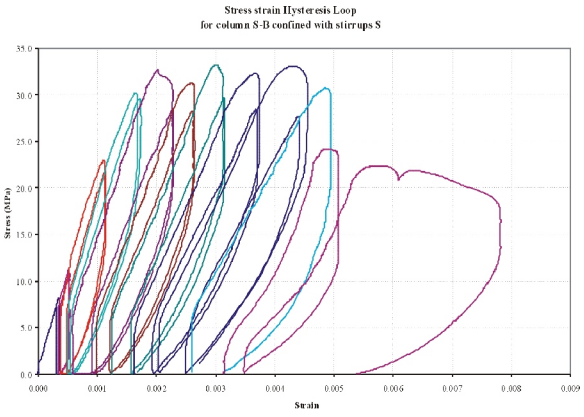

Fig. B2. Stress Strain Hysterisis Loops for column S-B

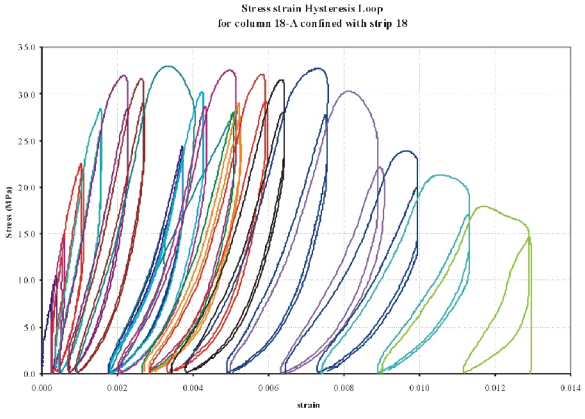

Fig. A5. Stress Strain Hysterisis Loops for column 18-A

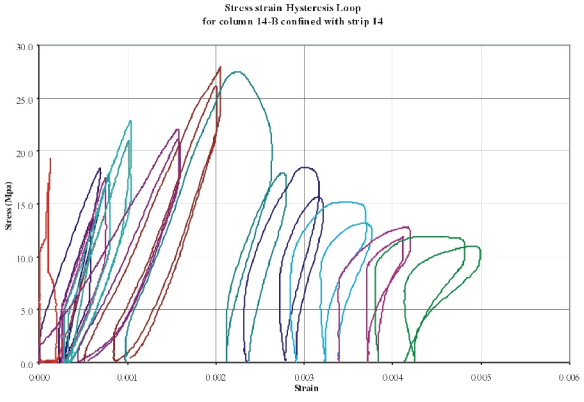

Fig. B3. Stress Strain Hysterisis Loops for column 14-B

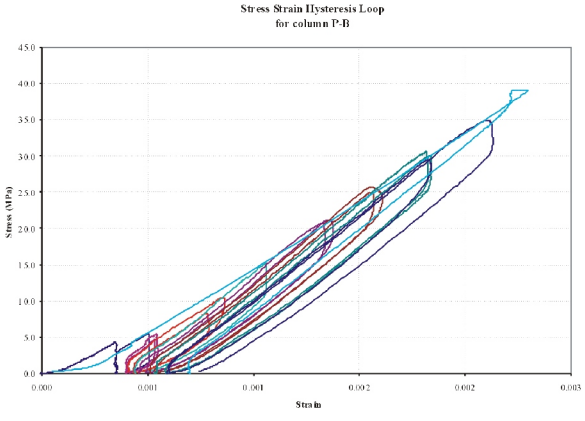

Fig. B1. Stress Strain Hysterisis Loops for column P-B

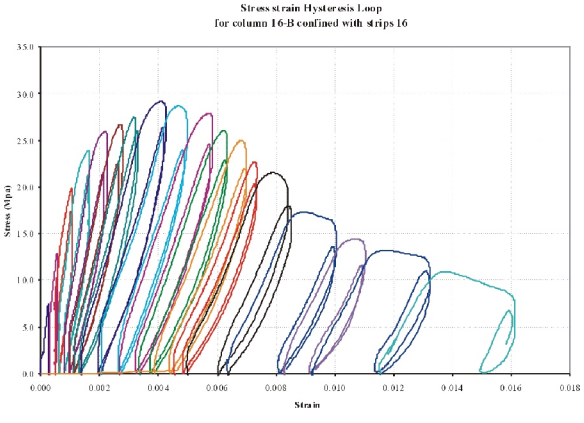

Fig. B4. Stress Strain Hysterisis Loops for column 16-B

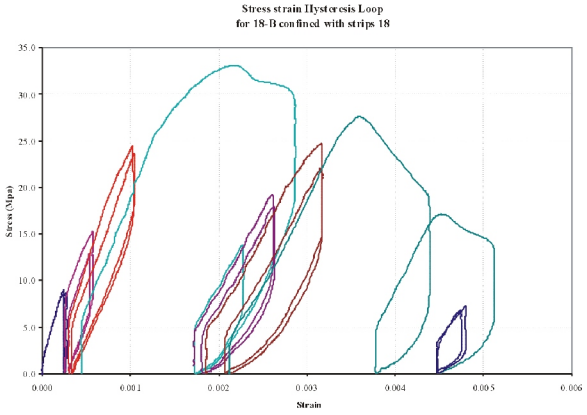

Fig. B5. Stress Strain Hysterisis Loops for column 18-B

Effect of Weld Current and Weld Speed on the Microstructure and Tensile Properties of Magnesium Alloy Specimens during Tungsten Inert Gas Welding

M. Abbas[1], A. Khan[2], M. Ali[3], M. A. Kamran[4], K. Azam[5], A. Shakoor[6]

[1,2,3,4,5,6]*University of Engineering and technology, Peshawar, Pakistan.*
[1]abbas_77us@yahoo.com

Abstract-Magnesium (Mg) and its alloys are considered the best materials for aerospace applications due its high strength to weight ratio[1]. In this paper, the effects of weld current and weld speed on the microstructures and mechanical properties of tungsten inert gas arc (TIG) welded magnesium alloy pieces were investigated by micro structural observations and tensile tests. The results showed that, the formation of porosity increased at higher values of weld current (170 & 180 A) and with further increase in the amount of the weld current (Heat input) the tendency of the formation of solidification cracking also increased. The ultimate tensile strength(UTS) of the samples increased with the increase in the weld current from 150 A to 160 A. However, a decrease in the value of ultimate tensile strength was observed when the current was further increased from 170 A to 180 A. At higher temperatures the Heat Affected Zone receives more heat, thus the grains grow faster under excessive heat and become coarse, resulting in a decrease in the UTS values. Samples were also welded using automatic mechanism with variable speeds ranging from 2 cm/sec to 4 cm/sec. Quality weld bead geometry was achieved at weld speed of 3.5 cm/sec, whereas, discontinuities were observed in samples prepared at 2, 2.5 and 4 cm/sec. The ultimate tensile strength of the welded samples at 3.5 cm/sec was higher than weldments at other welding speeds.

Keywords-TIG Welding, Weld Current and Speed, Magnesium Alloys.

I. INTRODUCTION

Magnesium alloys have a wide range of applications in the aerospace, automotive and electronic industry due to its light weight and high strength [2]. However, the wide applications of magnesium alloys needs improved weldability, since the production of complicated work pieces is difficult and expensive due to poor ductility of Mg alloys [3]. Problems, such as formation of coarse grains, oxidation, volatilization and thermal cracking, occur during welding as magnesium alloys have a low melting point, high thermal and electrical conductivity and large thermal expansion coefficient. Joining of Mg alloys requires extra care to obtain a sound weld with good quality [4]. The most common and widely applied method throughout the world for joining of Mg alloys is conventional Gas Tungsten Arc Welding (GTAW) [5]. These parts get deteriorated in service and require repair for achieving dimensional restorations. Tungsten inert gas (TIG) welding is usually preferred for Mg alloy parts during repair [6]. Welding defects and discontinuities are generally encountered during manual TIG welding. These discontinuities include porosity, voids, cracks (Hot cracking) and pin holes. Due to these defects critical Mg alloy parts fail to qualify the requisite quality checks/tests and get discarded [7]. Replacement of a discarded part with a new one is very expensive, whereas successful repair process is quite economical. To avoid discontinuities and obtain desirable weld bead geometry, selection of appropriate welding parameters is very important [8].

Welding input parameters play a very significant role in determining the quality of a weld joint. The joint quality can be defined in terms of properties such as weld-bead geometry, mechanical properties, and discontinuities [9]. Unfortunately, a serious problem during welding is the improper selection of input parameters which leads to discontinuities including lack of fusion, improper penetration, formation of pores, voids etc. [10]

Reference [11] performed TIG welding on Mg alloy AZ91D and observed hot cracking in the weld bead and Heat Affected Zone. Reference [12] observed that an increase in heat (welding current) leads to an increase in both the Heat Affected Zone and the grain size, on performing tests on AZ61 Mg alloy. Reference [13] performed manual tungsten inert gas welding on AZ61 Mg alloy and observed changes in the microstructure on varying the heat input. The increase in the heat input may cause low cooling rate for the Heat Affected Zone (HAZ) leading to formation of coarse

grains and hence porosities, cracks and discontinuities. Reference [14] in a set of experiments, performed on AZ61 Mg alloy, identified that effect of weld current initially increased the tensile properties, however at higher value of current tensile strenght was decreased. Reference [15] carried out experimental study on AZ91D Mg alloy and observed that the grain size increases when the welding speed is reduced and vice versa. It is clear from the above studies that the quality of a welded joint depends on the heat input, which is a function of the weld current, and weld speed. The work presented here is focused on determining the effect of weld current and weld speed on development of microstructures and mechanical properties of Mg alloys undergoing TIG welding.

II. Experimental Work and Methodology

Experimental work included manual and automatic TIG welding performed on the Mg alloy test pieces. Metallographic images were taken at 500x and 200x magnifications using "Leice DMI" 5000 metallurgical inverted microscope, in order to analyze the micro-structural behavior and metallurgical effects on the overall geometry of weld bead and heat affected zone. Moreover, tensile tests were performed to examine the mechanical properties of the material and weld strength, using tensile tester model "WAW-100B" capable to undertake metallic, non metallic samples and composites materials exposed to maximum of 100KN force. Chemical composition of the Mg alloy base material studied is given in Table I. GTH3Z2 BUILD-UP welding rod, with a diameter of 4 mm was used for welding of Mg alloy samples.

TABLE I
Chemical Composition of Mg Alloy By Wt %

Mg	*Th*	*Zn*	*Zr*	*Mn*
95%	*2.7%*	1.5%	0.5%	0.2%
Cu	*Si*	*Fe*	*Ni*	*Al*
0.03%	*0.01%*	0.01%	0.005%	0.045%

The quality of TIG weld greatly depends on the selection of appropriate process parameters. These parameters include welding current, welding speed, welding arc voltage, welding wire diameter, distance between arc and base material, shielding gas flow rate. TIG welding was performed on the Mg alloy test pieces in two phases. In the first phase, manual TIG welding was performed by keeping welding current as variable. During the second phase automatic speed controlled TIG welding was performed by taking weld speed as variable. A number of inspections including non-destructive as well as destructive tests were performed in accordance with American Welding Society AWS D17-1 and ISO 9001-C. The non-destructive tests included micro structural analysis (metallographic images) aimed to investigate the metallurgical changes, discontinuities like cracks, porosity, voids etc. in the weld heat affected zone. Another important test carried out was destructive inspection i-e tensile test to determine the strength of the test samples.

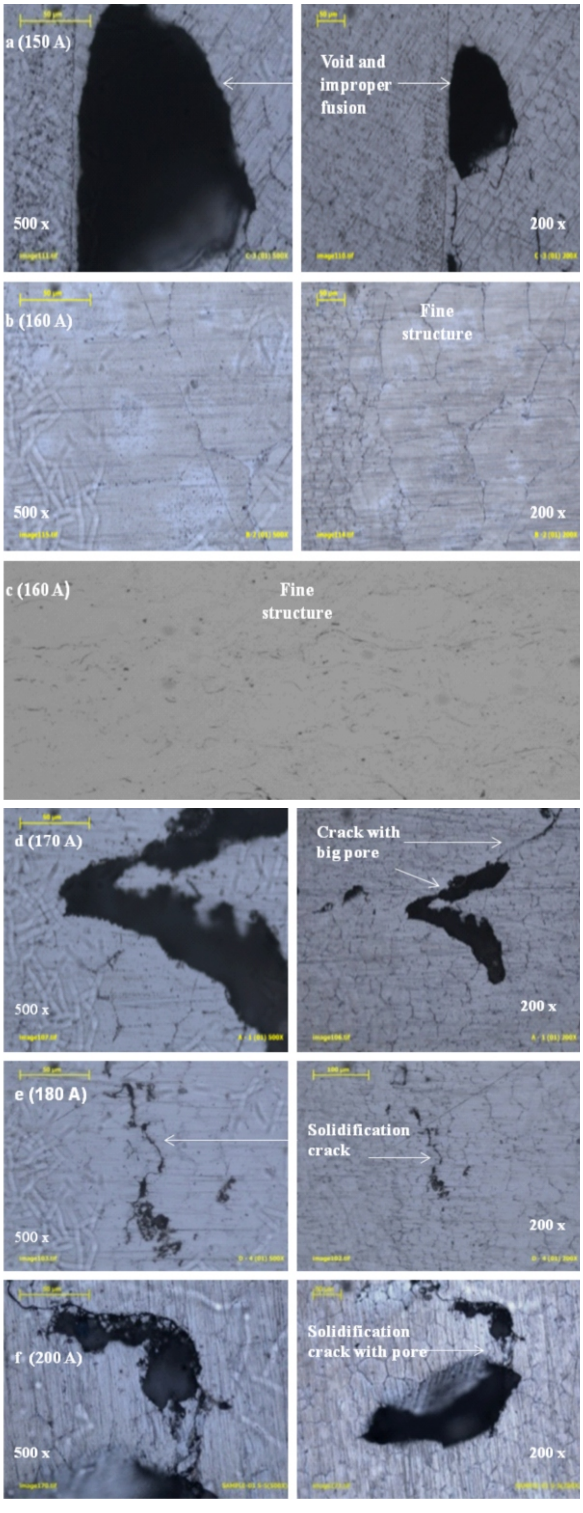

Fig. 1. Manual TIG welding at (a) 150, (b&c) 160, (d) 170, (e) 180 and (f) 200 A

III. OBSERVATIONS

Fig. 1. shows Metallographic images of Mg alloy samples welded manually at different weld currents. The Metallographic image in Fig.1 (a), welded at 150A, clearly shows lack of penetration and lack of fusion appearing just at the edge of weld bead in the heat affected zone which is adjacent to base metal, bifurcated by a thin visible line. The weld bead geometry in the area of HAZ has a coarse grain structure. This lack of penetration is caused due to relatively low current. The metallographic image in Fig.1 (b)&(c), welded at 160 A, revealed no discontinuities or defects. It is evident from these images that the grains of weld portion have fine structure and there is no evidence of presence of any discontinuities such as pores, voids, holes or cracks.

Further increase in the weld current to 170 A led to porosity spreading throughout the weld bead Fig.1(d). A large void was created and on the top side of the void, a number of clustered type porosities are clearly visible. A crater type crack is also visible which shows poor quality weld. For Mg alloy test piece welded at welding current of 180 A Fig.1(e), Clustered porosity is observed at different locations throughout the HAZ. A significant line has been observed which may be termed as solidification crack. For test piece welded at 200 A, micro structure showed a significant thick crack and porosities. The crack is a solidification type of crack. From the above experiments, the value of the best weld current can be determined as 160 A, since the sample welded at this current had no discontinuities and highest value of UTS. At higher current more heat is generated in the fusion zone and the grains get coarsen due to slow cooling rate which results in lower UTS values. Furthermore, excessive heat input at higher weld current values results in release of some stirred materials in the weld bead which produces flaws including cracks, pores etc.

Fig. 2. shows Mg alloy samples welded at weld current of 160 A, but at variable speeds. The metallographic image of Fig.2(a) illustrates a solid crack developed due to welding at slow speed (2 cm/sec). This is because more time is required to complete a pass at slow speed, resulting in large amount of heat received per unit length by the grains. A significant crack is visible in the weld which resulted due to excessive heat input. The Metallographic image in Fig.2(b) illustrates coarse grain size structure of Mg alloy specimen welded at weld speed of 2.5 cm/sec. There is no evident formation of cracks or defects like porosity and voids. At the edges of few grains granular flakes and dendrite growth is observed. Next Mg alloy piece was prepared with torch speed was set at 3.5 cm/sec. The metallographic image shown in Fig.2(c) has equiaxed grain structure extended from center of the image towards the right.

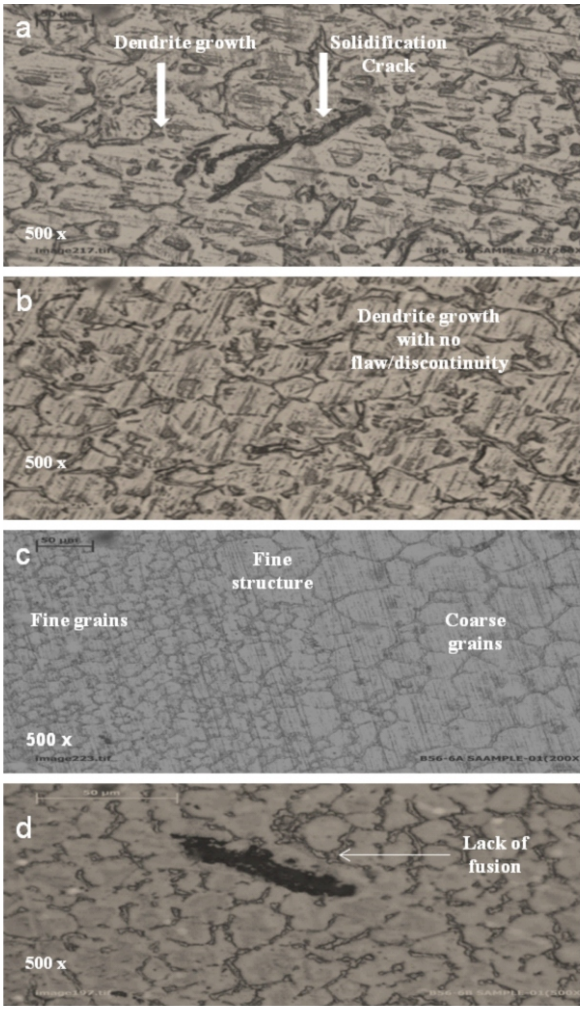

Fig. 2. Automatic TIG welding with weld current of 160 A and weld speeds of (a) 2, (b) 2.5 (c) 3 & (d) 4 cm/sec

The weld bead geometry from the center towards the left side of the image is even better and sound. It depicts properly oriented grains having fine crystal like structure. No discontinuities like voids, porosity or cracks are observed.

Metallographic result of Fig. 2(d) for Mg alloy sample welded at 160 A and weld speed of 4 cm/sec, illustrates lack of fusion with metallic inclusions welded at a relatively higher speed. Cellular dendrite is observed throughout the structure which is not properly oriented.

From the graph of Fig.3(a) it can be determined that at moderate welding current of 150A the value of tensile stress is 87.5 MPa, which increases to 95.8MPa when the current is increased to 160 A. The lowest value of UTS is at welding current of 180 A. The graph of Fig.3 (b) illustrates relationship between Tensile stress and weld speed.

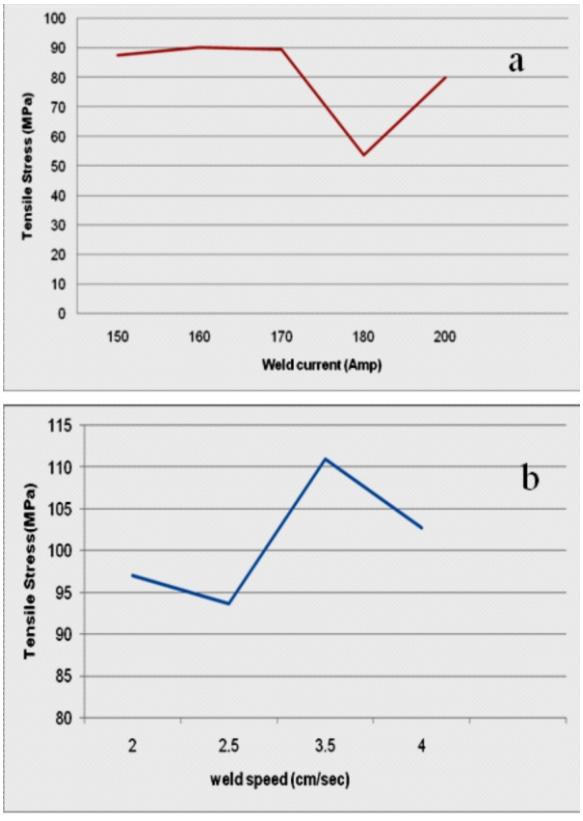

Fig. 3. UTS vs Weld current and Weld speed
(A) Manual welding (b) Automatic welding

It has been observed that UTS of the piece welded at a speed of 2 cm/sec is slightly higher than the strength of piece welded at 2.5cm/sec. When the speed is further increased to 3.5 cm/sec, UTS reached it maximum value of 111 MPa, however, when the speed is increased to 4cm/sec the UTS of the weld specimen dropped to a value of 102.7 MPa. At slow speeds there is more time available for the weld torch to deposit the molten material on to the substrate surface, thus the amount of heat energy generated and received by the grains at slow speeds is more per unit length, as more time is available to complete the pass.

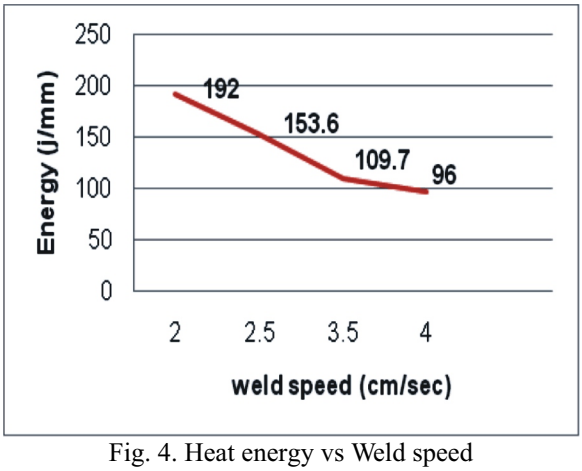

Fig. 4. Heat energy vs Weld speed

The graph in Fig.4 illustrates relationship between weld speed and heat energy produced during the process. It shows that with the increase in the speed the heat energy produced during the process decreases linearly. This shows that a linear relationship exists between weld speed and energy produced. At weld speed of 3.5cm/sec the amount of heat energy generated and received in the heat affected zone is 109.7 joules/mm at which a sound, stable and quality weld bead profile having better tensile strength has been obtained.

Due to excessive heat generation at slower weld speeds the possibility of discontinuities increases. The values of heat energy generated during the two slow speed processes at 2 and 2.5 cm/sec are 192 and 153.6 joules / mm. It is pertinent to mention that all the test pieces prepared by automatic welding speed had better results than the ones produced with manual welding.

IV. Conclusions

During manual TIG welding, at weld current of 150 A discontinuities like lack of penetration and improper fusion were observed. A sound and good quality weld bead was obtained at weld current of 160 A. At 170 A, moderate porosity, small voids and air traps have been observed in the weld bead heat affected zone of the test sample. Further increase in the amount of welding current(180 A) increased the heat input which consequently increased the amount of discontinuities porosities, pin holes, crater cracks and voids to a certain extent where those discontinuities were not acceptable and declared defects. An increase in the amount of welding current from 180 to 200 A increased the amount of weld discontinuities further. A significant crack was also observed in the Heat Affected Zone (HAZ) upon solidification of the molten metal. It may be termed as solidification crack. A decreasing trend in the values of UTS has been observed at 170, 180 and 200 A of current. The microstructure and mechanical properties of sample prepared by manual TIG welding by setting the value of welding current at 160 A showed best results having absolutely minimum amount of discontinuities. A sound quality of weld bead geometry with better mechanical properties having better UTS values of 95.6 MPa has been observed. Automatic TIG welding was done in the second phase by keeping optimal weld current value of 160 A and different weld speeds, 2cm/sec, 2.5cm/sec, 3.5cm/sec and 4cm/sec speeds were selected. At weld speed of 3.5cm/sec a sound, stable and quality weld bead profile was obtained which also had good mechanical properties as determined by the tensile testing. Test pieces welded with auto controlled variable speed have far better results than those produced manually. this is because a very smooth and precise passes were performed during auto mode that resulted in a fine weld bead goemetry. Moreover complete fusion and proper penetration is

also possible with smooth flow during welding pass, however same is not possible in manual welding.

REFERENCES

[1] G. Davies," Magnesium materials for automotive bodies", vol. 91, G. London; Elsevier, pp. 1327, 2003.

[2] K. U. Kainer, " Development of Magnesium applications" in Magnesium- Alloys and Technologies. WILEY-VCH Verlag GmbH & Co, Germany. pp. 12-18, 2003.

[3] S. Fleming, " An Overview of Magnesium based Alloys for Aerospace and Automotive Applications. M.S, Rensselaer Polytechnic Institute Hartford, CT, New York August, 2012.

[4] E. Aghion, B. Bronfin," Magnesium alloys development towards the 21st century", Magnesium alloys. Material Science Forum 2000.

[5] F. Czerwinski, Welding and Joining of Magnesium Alloys, Magnesium Alloys - Design, Processing and Properties.2011.

[6] M. K. Kulekci (2007, Nov) Magnesium and its alloys applications in automotive industry. Springer-verlag Ltd. International Journal of Advanced Manufactruing Technology 39. pp. 851-866.

[7] L. Liu," Welding metallurgy of magnesium alloys" in Welding and joining of magnesium alloys. Woodhead Publishing Limited, Abington Hall, Granta Park, Great Abington, Cambridge, UK. pp. 11-14, 2010.

[8] J. F. Lancaster, Metallurgy of Welding Magnesium Alloys, 5th ed. Chapman & Hall Incorporation, London,1993.

[9] C. T. Chi, C. G. Chao, T. F. Liu and C. C. Wang, Relational analysis between parameters and defects for electron beam welding of AZ-series of magnesium alloys Published by Elsevier Ltd. Vol 30. pp. 23-34, 2008.

[10] L. Wang, H. Rhee, S. D. Felicelli. Porosity defects and oxide films in magnesium alloy AZ91. Shape casting: the 3rd international symposium. The minerals, metals and materials society, 2009.

[11] W. Zhou*, T. Z. Long and C. K. Mark. Hot cracking in tungsten inert gas welding of magnesium alloy AZ91D. materials science and technology, vol 23, 2007.

[12] W. Zhe, L. Dao-gang, W. Guo-ping. Analysis of structure and property of cast Mg alloy AZ91 weld joints. Modern Welding, 2008.

[13] D. Min, J. Shen, S. Lai, J. Chen. Effect of heat input on the microstructure and mechanical properties of tungsten inert gas arc butt-welded AZ61 magnesium alloy plates.. Journal of Materials characterization Elsevier Ltd Inc, vol. 60. pp. 1583-1590, 2009.

[14] A. R. Rose, Prediction and optimization of pulsed current tungsten inert gas welding parameters to attain maximum tensile strength in AZ61A magnesium alloy. Journal of Materials and Design Elsevier Ltd, vol. 37. pp. 334-338, 2012.

[15] A. Munitz, C. Cotler, A. Stern, G. Kohn, Mechanical properties and microstructure of gas tungsten arc welded magnesium AZ91D plates. Mater Sci Eng, vol. 302. pp. 6873, 2001.

Development of Compressive Strength for Concrete with Different Curing Durations

A. Latif [1], M. U. Rashid[2], K. Kheder[3], T. Sultan[4], F. Mehvish[5]

[1,4,5]Department of Civil Engineering, University College of Engg. & Tech. BZU. Multan, Pakistan
[2]Senior Engineer, WR Division, NESPAK, Lahore, Pakistan
[3]Department of Civil Engineering, College of Engineering, Salman bin Abdul Aziz University, P. O. Box 655, AlKharj 11942 Saudi Arabia
[1]engrabid1997@gmail.com

Abstract-Durability and properties of concrete are deliberately affected by curing process which also influences the hydration process of cement. The whole effort is being carried out to study the "Effect of curing duration on compressive strength of concrete" by using British and American standard specimens. By proper curing concrete perform well for all the design life of the structure. In our study, all other parameters (W/C ratio, Temperature, Material, curing method) that can affect the strength of concrete kept constant except curing durations. The Variable parameter of the study includes the curing durations (7, 14, 21, 28, 60 and 90 days). To achieve the aim of this study total 72 cubes and cylinders specimens were cast with OPC (Ordinary Portland cement). Half of Specimens (Cubes and Cylinders) are placed in a water tank and remaining half are placed in air before testing (compression strength test). The results of tests indicate a decrease in compressive strength for all duration of uncured cubes and cylinders as compared to cured cubes and cylinders that indicate good results. The majority of the cubes and cylinders tested, showed a significant improvement in compressive strength by increasing the duration of curing.

Keywords-Compressive strength, duration, curing, hydration process, OPC (Ordinary Portland cement)

I. Introduction

This paper addresses the impact of improper curing in reducing the properties and compressive strength of concrete. In Pakistan and developing countries, proper curing of concrete is usually neglected at construction sites and very few organizations get the advantages of proper curing of concrete. Construction is very important in any community of the world and concrete is a material through which desire shape of structures are acquired. The hydration process of cement stops when relative humidity decreases below 80% but due to an efficient curing such as water curing the decrease of relative humidity can be controlled [1-2]. Proper curing is essential primarily to keep the concrete moist during the strength gaining process [3]. Proper Curing is act as a tool to control the rate of evaporation during hydration process from concrete [4-6].

In arid to semi-arid countries evaporation occurs at higher rates due to high temperature/wind, which decreases the amount of available moisture by reducing the relative humidity and retarding the process of hydration for cement. In severe circumstances, hydration process of cement is eventually stopped. When the hydration is stopped, sufficient calcium silicate hydrate (CSH) cannot develop from the reaction of cement compounds and water which is the major product of cement hydration providing strength and proper curing is only the technique to develop the adequate amount of CSH [7-8].

This study presents the effect of curing on hardened properties such as compressive strength. The cured and uncured samples have been compared to investigate its effect at different ages i.e. 7, 14, 21, 28, 60 and 90 days.

II. Methodology

Several methods of curing are as follows:

Water curing.

Wrapped curing.

Dry-air curing.

The most convenient option is water curing and considered for the study. The conventional curing involves dipping the specimens in water at 25 C^0 at the end of 24 hours of casting after allowing for air drying. Two types of specimens i.e. cubes and cylinders according to British and American standards were used for curing and comparing results respectively. According to standards material statement was prepared and accordingly the cement, fine and course aggregates were used for casting of the cylinders and cubes. While selecting materials, the following general precautions considered.

Newly stocked cement

Well graded fine and coarse aggregates

The required tests were performed to check the suitability and characteristics of concrete ingredients. The material fulfilled the criterion were finally selected for preparing concrete and casting cubes and cylinders. Compaction was done by using vibrating table and other criterion to avoid segregation and bleeding etc. were also taken under consideration. Specimens were cured in water pond as shown in Fig. 1 and finally tested to drive the required effects and results of compressive strength of different duration. Cubes and cylinders according to British and American standards respectively, were casted to check the compressive strength of the concrete. Necessary precautions were observed at all the stages of the study.

Fig. 1. Curing pond for specimens

Compression strength was determined by using compression testing machine, presented in Fig. 2, for each cured and uncured cube and cylinder specimen. Load applied is noted directly from the computer screen of the compression testing machine and compressive strength is calculated by using the following relation:

$$\text{Compressive strength} = \frac{\text{Load Applied by machine}}{\text{Area of Cube/Cylinder}}$$

The concrete mix materials used in the study are shown in Table I.

III. Test Results and Discussions

The current study on different curing durations verifies that proper curing of concrete can achieve higher compressive strength due to the less extent of moisture loss and greater degree of hydration process.

TABLE I
Concrete Mix Materials

No.	Description of materials	Source of materials
1	Fine aggregate	Chenab sand
2	Coarse aggregate	Sakhi-Sarwar crush
3	Cement	D.G Cement
4	Water	Tab water (drinkable)

Fig. 2. Testing of specimen in compression testing machine

The test results of all the concrete cubes and cylinders are summarized in Table II and Table III, whereas their graphical representation is shown in Fig. 3 and Fig. 4 respectively. The results and discussions regarding to compressive strength of cubes and cylinders with and without curing have been elaborated as follows:

The compressive strength of concrete cubes and cylinders having proper curing was higher than the uncured concrete cubes at 7, 14, 21, 28, 60 and 90 days curing ages as shown in Fig. 3 and Fig. 4.

The increase of avg. compressive strength for cubes from 7 days to 14 days, 14 days to 21 days, 21 days to 28 days, 28 days to 2 months and 2 months to 3 months is 168 psi, 341 psi and 221 psi, 165.7 psi and 65.5 psi respectively.

TABLE II
SUMMARIZED RESULTS OF COMPRESSION TEST FOR CURED AND UNCURED CUBES SAMPLES

Curing Duration	Sample No.	Cured Cubes Samples		Sample No.	Uncured Cubes Samples		Rate of Increment in Strength	
		Compressive Strength	Average Compressive Strength		Compressive Strength	Average Compressive Strength	Increment	%Age
Days		psi	psi		psi	psi	psi	%
7	1	3004.54	2982.79	4	2897.75	2617.72	365.08	12
	2	2994.98		5	2526.01			
	3	2948.86		6	2429.39			
14	7	3094.15	3003.14	10	2907.68	2804.95	198.19	7
	8	2954.45		11	2844.16			
	9	2960.82		12	2663.00			
21	13	3508.42	3487.65	16	3402.34	3272.40	215.25	6
	14	3483.14		17	3246.48			
	15	3471.40		18	3168.39			
28	19	3618.47	3468.08	22	3367.11	3170.42	297.65	9
	20	3496.90		23	3130.74			
	21	3288.86		24	3013.42			
60	25	3779.56	3504.37	28	3482.63	3280.52	223.86	6
	26	3527.63		29	3354.11			
	27	3205.93		30	3004.80			
90	31	3870.78	3671.59	34	3482.63	3280.51	391.08	11
	32	3527.60		35	3354.11			
	33	3616.39		36	3004.80			

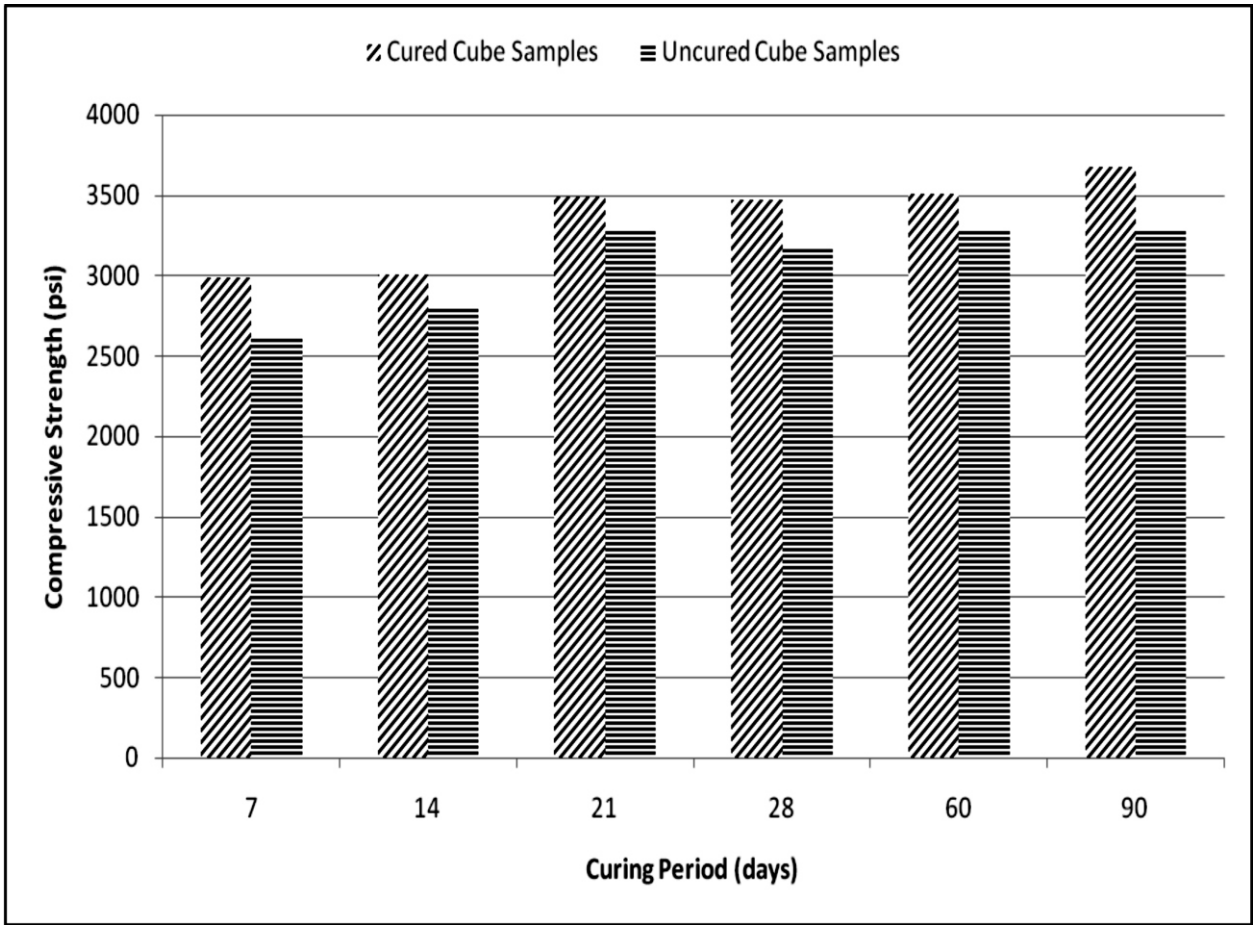

Fig. 3. Graphical representation of comparison of cured and uncured cubes

TABLE III
RESULTS OF COMPRESSION TEST FOR CURED AND UNCURED CYLINDER SAMPLES

Curing Duration	Sample No.	Cured Cylinder Samples		Sample No.	Uncured Cylinder Samples		Rate of Increment in Strength	
		Compressive Strength	Average Compressive Strength		Compressive Strength	Average Compressive Strength	Increment	%Age
Days		psi	psi		psi	psi	psi	%
7	1	2090.58	1887.39	4	1611.85	1492.94	394.46	21
	2	1805.62		5	1497.35			
	3	1765.98		6	1369.63			
14	7	2041.23	2100.58	10	1953.15	1841.59	258.99	12
	8	2098.15		11	1995.00			
	9	2162.38		12	1576.63			
21	13	2492.65	2315.02	16	2091.87	1959.03	355.99	15
	14	2397.95		17	1935.54			
	15	2054.46		18	1849.68			
28	19	2762.27	2661.71	22	2316.94	2022.27	639.44	24
	20	2729.89		23	2153.94			
	21	2492.97		24	1595.93			
60	25	3083.56	2805.66	28	2411.50	2172.26	633.40	23
	26	2764.62		29	2154.83			
	27	2568.80		30	1950.46			
90	31	3156.88	2905.25	34	2572.30	2300.08	605.18	21
	32	2916.61		35	2252.61			
	33	2642.27		36	2075.33			

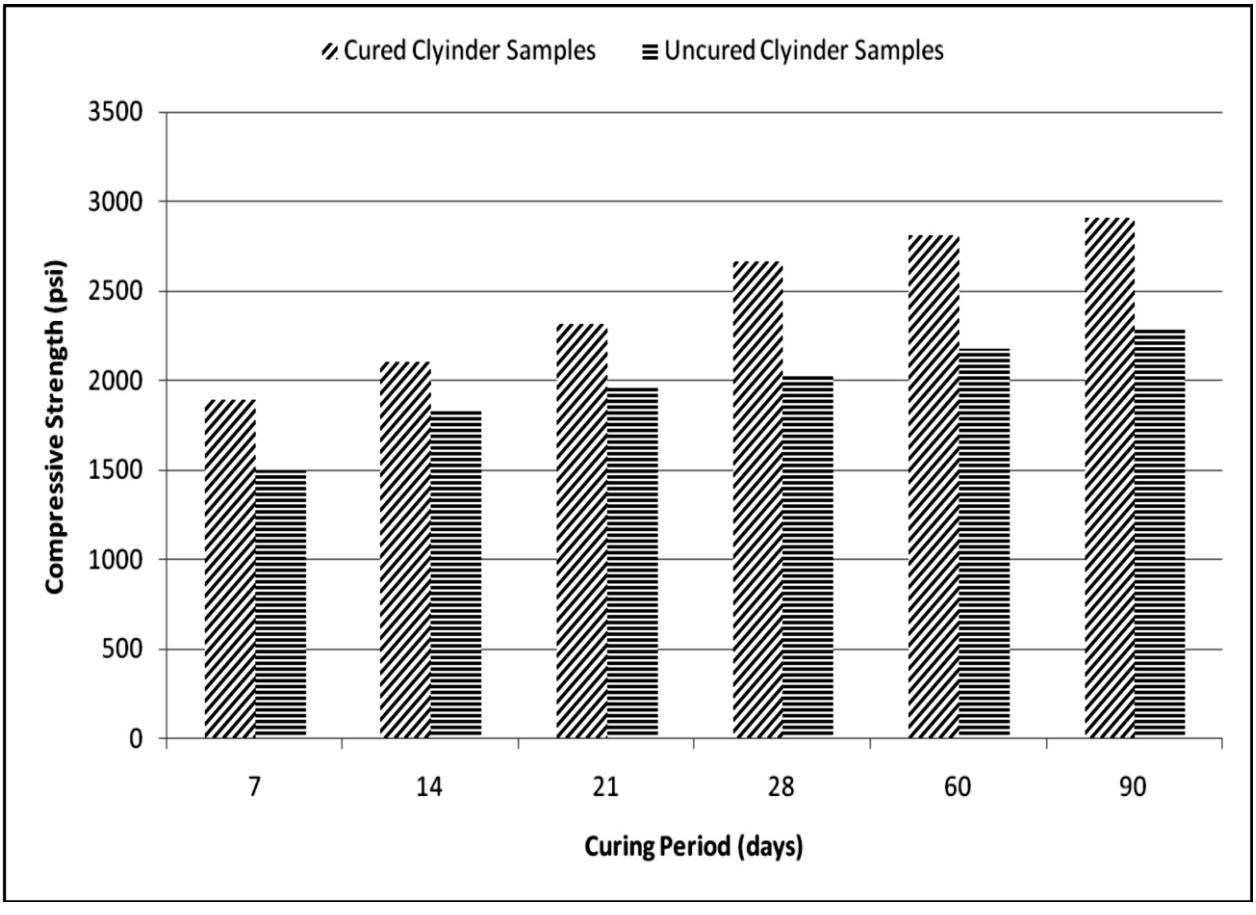

Fig. 4. Graphical representation of comparison of cured and uncured cylinders

The increase of average compressive strength for cylinders from 7 days to 14 days, 14 days to 21 days, 21 days to 28 days, 28 days to 2 months and 2 months to 3 months is 367 psi, 314.5 psi, 237 psi, 253 psi, and 203 psi respectively.

It can be seen that there is increase in strength with the increase in curing duration. This increase in strength due to proper curing shows the availability of moisture for hydration process. For all durations, the maximum average compressive strength of cured concrete samples is 12% higher than uncured samples.

The rate of increase of average compressive strength for cubes due to curing from 7 days to 14 days, 14 days to 21 days, 21 days to 28 days, 28 days to 2 months and 2 months to 3 months is in ranges of 7%, 18%, 31%, 46%, 62% and 62% respectively.

The rate of increase of average compressive strength for cylinders due to curing from 7 days to 14 days, 14 days to 21 days, 21 days to 28 days, 28 days to 2 months and 2 months to 3 months is 9%, 13%, 15%, 21% , 23% and 24% respectively.

IV. Conclusions

It is important to know that all the theoretical and practical values of compressive strength are calculated at the point of complete failure. The conclusions of the study are as follows:

Compressive strength of cured samples is much higher than uncured samples.

The compressive strength of concrete can be increased by enhancing the curing duration up to a certain limit.

The age of concrete plays an important role for compressive strength. As the age increases, the compressive strength of concrete also increases for both the cured and uncured samples**.**

In uncured samples, the moisture escapes from the specimens that increase porosity and reduces compressive strength of concrete.

Curing needs care in hot weather condition. Minimum 28 days curing for plain cement concrete is recommended and at least 14 days curing should be done at all construction projects.

V. Recommendations

In this study, curing is done by conventional method, further, it is recommended that the study can be carried out by changing the curing method (wrapped curing/dry-air curing) and checked its effects on compressive strength of concrete.

References

[1] A. M. Neville, "Properties of Concrete", 4th Edition, Pitman Publishing Limited, London 1997.

[2] H. Nilson, D. Darvin, C. W. Dolan, “Design of Concrete Structures”, Thirteenth Edition, Shear and Diagonal Tension in beams.

[3] *Cement Concrete & Aggregates Australia Data Sheet*, published by CCAA, 2006, pp. 1-7.

[4] M. V. K. Rao, P. R. Kumar and A. M. Khan 2010 “A study on the influence of curing on the strength of a standard grade concrete mix” Series: Architecture and Civil Engineering Vol. 8, No. 1, 2010, pp. 23-34.

[5] M. Safiuddin, S. N. Raman and M. F. M. Zain, "Effect of Different Curing Methods on the Properties of Micro silica Concrete", Australian journal of Basic and Applied Sciences, 1 (2), 2007, pp. 87-95.

[6] H. M. Tantawi and E. S. Gharaibey, "Early estimation of Hardened Concrete Strength", journal of the Applied Sciences, 6 (3), 2006, pp. 543-547.

[7] M. Shoba and P. S. N. Raju, "Effect of Curing Compound on different Concretes", New Building materials and construction world, vol-11, issue-4, October 2005, pp. 66-71.

[8] P. R. Oliveira, A. L. B. Geyer, and A. Liduario, "Application of Different Curing Procedures in High-Performance Concrete (HPC)", ACI journal, Vol. 229, September 2005, pp. 165-174.

Technical Journal
University of Engineering and Technology, Taxila
Website: www.uettaxila.edu.pk.

CALL FOR PAPERS

Researchers and Academia are invited to submit the research articles to Technical Journal of UET Taxila. It is a broad-based open access journal. It covers all areas of science, engineering and management.

Technical Journal is a quarterly publication of UET Taxila recognized by HEC in "Y" category. It is published regularly with a key objective to provide the visionary wisdom to academia and researchers to disseminate novel knowledge and technology for the benefit of society. Technical Journal is indexed by well recognized international database such as PASTIC Science Abstracts, AGRIS Data Base and ProQuest Products.

For enquiries, submissions of articles or any other information please visit our website http://web.uettaxila.edu.pk or contact the Editorial Office on the following numbers:

+92-51-9047455, +92-51-9047298
E-mail: technical.journal@uettaxila.edu.pk

It will be highly appreciated if the information is forward to interested colleagues from Pakistan as well as abroad.

Looking forward to receiving the research papers on behalf of Technical Journal Editorial Office.

Prof. Dr. Abdul Razzaq Ghumman
Chief Editor
Technical Journal,
UET, Taxila

Instruction for authors for publishing in Technical Journal UET Taxila

1. Font size must be 10 Times New Roman.
2. Define abbreviations and acronyms the first time they are used in the text, even after they have already been defined in the abstract. Do not use abbreviations in the title unless they are Unavoidable
3. Use zero before decimal places: "0.24" not ".24".
4. Avoid contractions; for example, write "do not" instead of "don't."
5. If you are using *Word,* use either the Microsoft Equation Editor or the *MathType* add-on (http://www.mathtype.com) for equations in your paper (Insert | Object | Create New | Microsoft Equation *or* MathType Equation). Number equations consecutively with equation numbers in parentheses flush with the right margin, as in (1).
   Refer to "(1)," not "Eq. (1)" or "equation (1)," except at the beginning of a sentence: "Equation (1) is ... ."
6. Symbols used in the equations must be defined before or immediately after it appears.
7. Use SI units only.
8. All figures should be at least 300dpi.
9. When referencing your figures and tables within your paper, use the abbreviation "Fig." Even at the beginning of a sentence. Do not abbreviate "Table." Tables should be numbered with Roman Numerals.
10. Reference may be cited with number in square brackets, e.g. "the scheme is discussed in [3]". Multiple references are each numbered with separate brackets. Do not use "Ref." or "reference" except at the beginning of a sentence: "Reference [11] illustrates... ." Please do not use automatic endnotes in Word, rather, type the reference list at the end of the paper using the "References" style.

Note: For template of paper please visit our journal's page: http://web.uettaxila.edu.pk/techjournal/index.html